

CANCER DISCOVERY

AZD9291, an Irreversible EGFR TKI, Overcomes T790M-Mediated Resistance to EGFR Inhibitors in Lung Cancer

Darren A.E. Cross, Susan E. Ashton, Serban Ghiorghiu, et al.

Cancer Discovery Published OnlineFirst June 3, 2014.

Updated version Access the most recent version of this article at:
doi:[10.1158/2159-8290.CD-14-0337](https://doi.org/10.1158/2159-8290.CD-14-0337)

Supplementary Material Access the most recent supplemental material at:
<http://cancerdiscovery.aacrjournals.org/content/suppl/2014/06/03/2159-8290.CD-14-0337.DC1.html>

E-mail alerts [Sign up to receive free email-alerts](#) related to this article or journal.

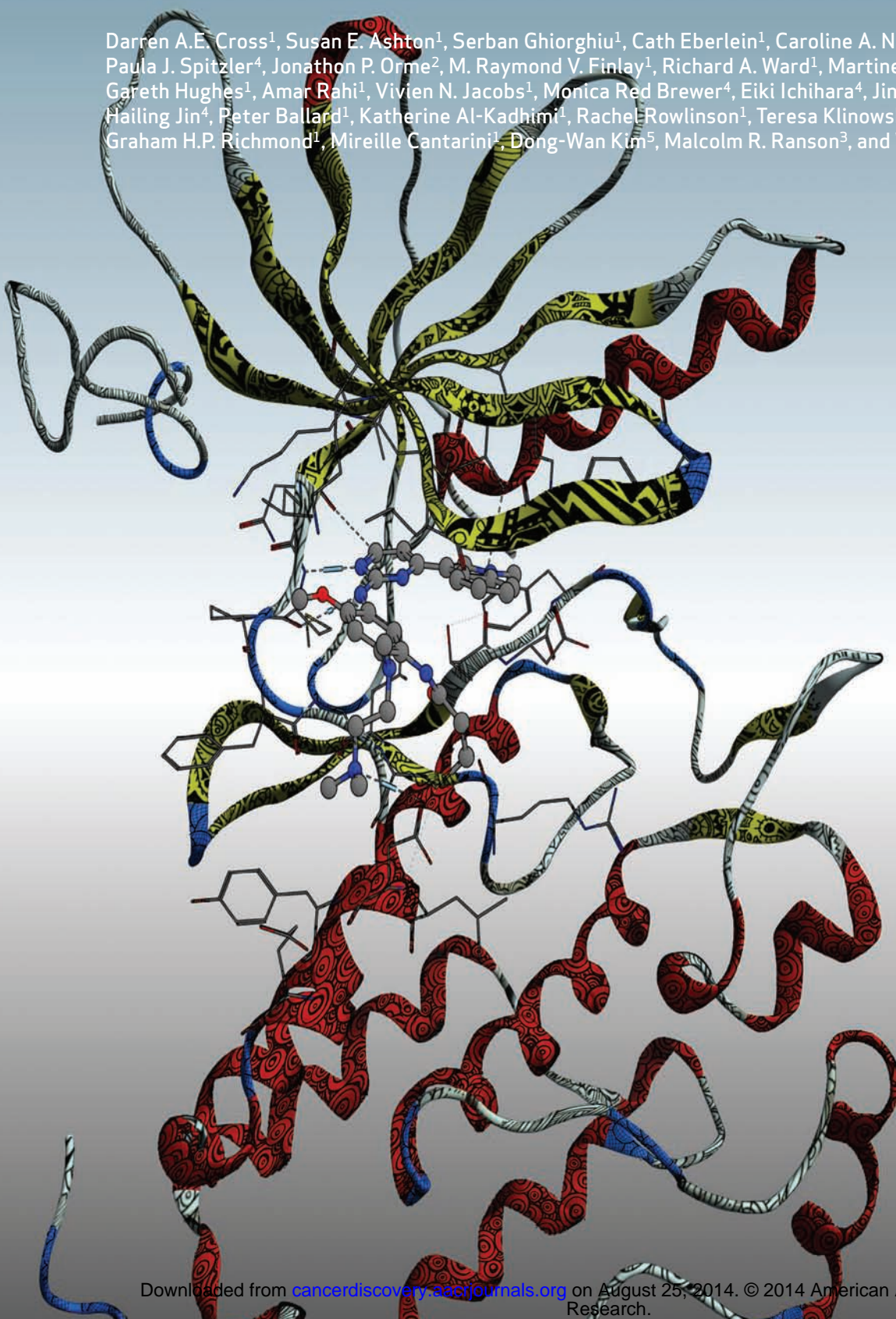
Reprints and Subscriptions To order reprints of this article or to subscribe to the journal, contact the AACR Publications Department at pubs@aacr.org.

Permissions To request permission to re-use all or part of this article, contact the AACR Publications Department at permissions@aacr.org.

RESEARCH ARTICLE

AZD9291, an Irreversible EGFR TKI, Overcomes T790M-Mediated Resistance to EGFR Inhibitors in Lung Cancer

Darren A.E. Cross¹, Susan E. Ashton¹, Serban Gheorghiu¹, Cath Eberlein¹, Caroline A. Nebhan⁴, Paula J. Spitzler⁴, Jonathon P. Orme², M. Raymond V. Finlay¹, Richard A. Ward¹, Martine J. Mellor¹, Gareth Hughes¹, Amar Rahi¹, Vivien N. Jacobs¹, Monica Red Brewer⁴, Eiki Ichihara⁴, Jing Sun⁴, Hailing Jin⁴, Peter Ballard¹, Katherine Al-Kadhimi⁴, Rachel Rowlinson¹, Teresa Klinowska¹, Graham H.P. Richmond¹, Mireille Cantarini¹, Dong-Wan Kim⁵, Malcolm R. Ranson³, and William Pao⁴



ABSTRACT

First-generation EGFR tyrosine kinase inhibitors (EGFR TKI) provide significant clinical benefit in patients with advanced *EGFR*-mutant (*EGFRm*⁺) non-small cell lung cancer (NSCLC). Patients ultimately develop disease progression, often driven by acquisition of a second T790M *EGFR* TKI resistance mutation. AZD9291 is a novel oral, potent, and selective third-generation irreversible inhibitor of both *EGFRm*⁺ sensitizing and T790M resistance mutants that spares wild-type *EGFR*. This mono-anilino-pyrimidine compound is structurally distinct from other third-generation *EGFR* TKIs and offers a pharmacologically differentiated profile from earlier generation *EGFR* TKIs. Preclinically, the drug potently inhibits signaling pathways and cellular growth in both *EGFRm*⁺ and *EGFRm*⁺/T790M⁺ mutant cell lines *in vitro*, with lower activity against wild-type *EGFR* lines, translating into profound and sustained tumor regression in *EGFR*-mutant tumor xenograft and transgenic models. The treatment of 2 patients with advanced *EGFRm*⁺ T790M⁺ NSCLC is described as proof of principle.

SIGNIFICANCE: We report the development of a novel structurally distinct third-generation *EGFR* TKI, AZD9291, that irreversibly and selectively targets both sensitizing and resistant T790M⁺ mutant *EGFR* while harboring less activity toward wild-type *EGFR*. AZD9291 is showing promising responses in a phase I trial even at the first-dose level, with first published clinical proof-of-principle validation being presented. *Cancer Discov*; 4(9); 1–16. ©2014 AACR.

INTRODUCTION

Gefitinib (1) and erlotinib (2) are reversible small-molecule ATP analogues originally designed to inhibit the tyrosine kinase (TK) activity of wild-type *EGFR*. During their clinical development, these first-generation TK inhibitors (TKI) were serendipitously found to be most effective in patients with advanced non-small cell lung cancer (NSCLC) whose tumors harbor recurrent somatic activating mutations occurring in the exons encoding the kinase domain of *EGFR*, i.e., small multinucleotide in-frame deletions in exon 19 (ex19del) and a point mutation in exon 21 leading to substitution of leucine for arginine at position 858 (L858R; refs. 3–5). Tumors with these activating mutations (*EGFRm*⁺) account for approximately 10% to 15% and 40% of NSCLC in Western and Asian populations, respectively (6). Unfortunately, although patients with *EGFRm*⁺ tumors typically show good initial responses to first-generation TKIs, most patients who respond to therapy ultimately develop disease progression after about 9 to 14 months of treatment (7–11). Furthermore, these first-generation TKIs are associated with side effects

that include skin rash and diarrhea that are due to the inhibition of wild-type *EGFR* in skin and gastrointestinal organs (12).

Preclinical modeling and analysis of tumor tissue obtained from patients after the development of disease progression have led to the identification of a number of mechanisms that mediate *EGFR* TKI resistance. Such genetic and other signaling aberrations that drive resistance mechanisms include *HER2* amplification (13), *MET* amplification (14, 15), *PIK3CA* mutation (16), *BRAF* mutation (17), *NFI* loss (18), and potentially FGFR signaling (19). In addition, resistant tumors have also been reported to show histologic changes such as small-cell lung cancer (SCLC) transformation or epithelial-to-mesenchymal transition (EMT; ref. 16). However, it is now well established that acquisition of a second mutation in *EGFR*, resulting in substitution of threonine at the “gatekeeper” amino acid 790 to methionine (T790M), is the most common resistance mechanism and is detected in tumor cells from more than 50% of patients after disease progression (20, 21). The T790M mutation is believed to render the receptor refractory to inhibition by these reversible *EGFR* TKIs through exerting effects on both steric hindrance (22) and increased ATP affinity (23).

Current targeted therapeutic strategies for patients with acquired resistance are limited. Second-generation irreversible *EGFR* TKIs such as afatinib (24) and dacomitinib (25) are effective in untreated *EGFR*-mutant lung cancer (26, 27). However, as monotherapy, they have failed to overcome T790M-mediated resistance in patients (28, 29), because concentrations at which these irreversible TKIs overcome T790M activity preclinically are not achievable in humans due to dose-limiting toxicity related to nonselective inhibition of wild-type *EGFR* (30). Furthermore, these inhibitors can drive resistance through acquisition of T790M *in vitro* (31) and in patients (32), providing supportive evidence that they have low potency against T790M. One regimen that showed potential activity is afatinib

Authors' Affiliations: ¹Oncology Innovative Medicines and ²Discovery Sciences, AstraZeneca, Macclesfield Cheshire; ³University of Manchester, Christie Hospital, Manchester, United Kingdom; ⁴Department of Medicine and Vanderbilt-Ingram Cancer Center, Vanderbilt University, Nashville, Tennessee; and ⁵Seoul National University Hospital, Seoul, Republic of Korea

Note: Supplementary data for this article are available at Cancer Discovery Online (<http://cancerdiscovery.aacrjournals.org/>).

Corresponding Authors: Darren Cross, AstraZeneca, Alderley Park, Macclesfield SK10 4TG, United Kingdom. Phone: 44-1625-515649; E-mail: Darren.Cross@astrazeneca.com; and William Pao, Vanderbilt-Ingram Cancer Center, 2220 Pierce Avenue, 777 PRB, Nashville, TN 37232. Phone: 615-343-9454; Fax: 615-343-7602; E-mail: william.pao@vanderbilt.edu.

doi: 10.1158/2159-8290.CD-14-0337

©2014 American Association for Cancer Research.

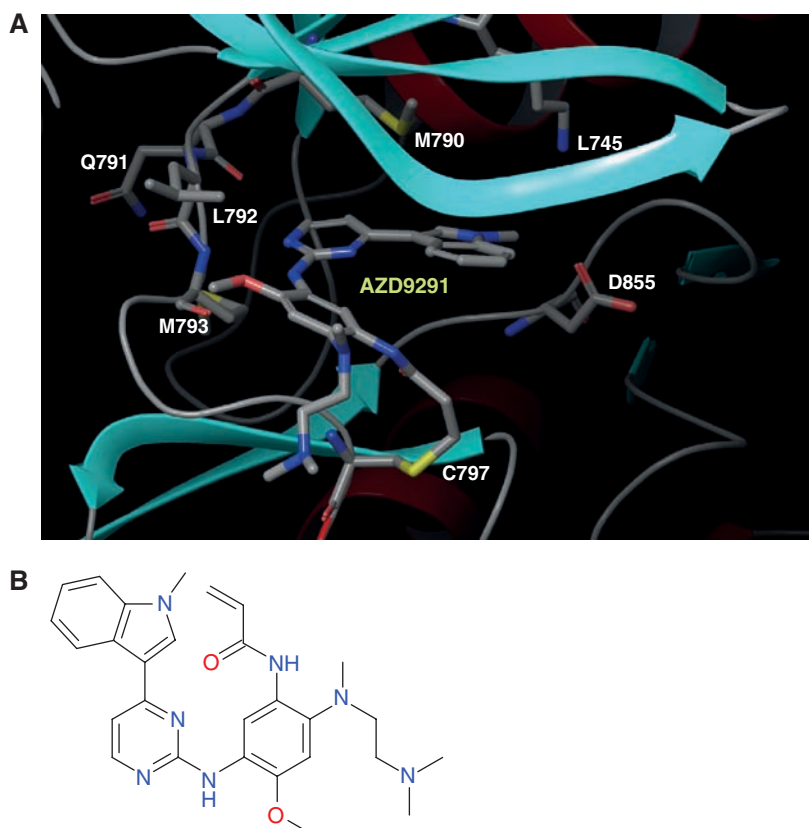


Figure 1. AZD9291 binding mode and structure. **A**, structural model showing the covalent mode of binding of AZD9291 to EGFR^{T790M} via Cys797. Shown is the pyrimidine core forming two hydrogen bonds to the hinge region (Met793), orientation of the indole group adjacent to the gatekeeper residue, the amine moiety positioned in the solvent channel, and the covalent bond formed to Cys797 via the acrylamide group of AZD9291. **B**, chemical structure of AZD9291.

plus the anti-EGFR antibody cetuximab, which induced a 29% confirmed response rate in a phase IB trial for patients with EGFR^{m+} lung cancer and acquired resistance to erlotinib (33). However, this combination has substantial skin toxicity, with 20% of patients reporting Common Terminology Criteria for Adverse Events (CTCAE) grade 3 or higher rash (33).

Therefore, there remains a significant unmet need for an EGFR TKI agent that can more effectively target T790M tumors while sparing the activity of wild-type EGFR. This has led to the development of “third-generation” EGFR TKIs that are designed to target T790M and EGFR TKI-sensitizing mutations more selectively than wild-type EGFR. WZ4002 was the first such agent to be published (34), although it has not progressed to clinical trials. A second agent closely related to the WZ4002 series, CO-1686, has been recently reported (35) and is currently in early phase II clinical trials. HM61713 is another “third-generation” agent that is currently in early phase I trials.

Here, we describe identification, characterization, and early clinical development of AZD9291, a novel, irreversible, EGFR TKI with selectivity against mutant versus wild-type forms of EGFR. AZD9291 is a mono-anilino-pyrimidine compound that is structurally and pharmacologically distinct from all other TKIs, including CO-1686 and WZ4002.

RESULTS

AZD9291 Is a Mutant-Selective, Irreversible Inhibitor of EGFR Kinase Activity

AstraZeneca developed a novel series of irreversible, small-molecule inhibitors to target the sensitizing and T790M-

resistant mutant forms of the EGFR tyrosine kinase with selectivity over the wild-type form of the receptor. These compounds bind to the EGFR kinase irreversibly by targeting the cysteine-797 residue in the ATP binding site via covalent bond formation (36), as depicted in the modeled structure for AZD9291 (Fig. 1A). Further work on this chemotype allowed additional structure activity relationships (SAR) to be discerned that enabled target potency to be increased without driving increased lipophilicity, thus maintaining favorable drug-like properties. Continued medicinal chemistry efforts achieved further improvements, including increased kinase selectivity, ultimately arriving at the mono-anilino-pyrimidine AZD9291 (Fig. 1B). Mass spectrometry of chymotrypsin digests confirmed that AZD9291 can covalently modify recombinant EGFR (L858R/T790M) at the target cysteine 797 amino acid (Supplementary Fig. S1A and S1B).

AZD9291 has a distinct chemical structure from the other third-generation TKIs, WZ4002 (34) and CO-1686 (35). Although the former two compounds share a number of common structural features [e.g., positioning of the electrophilic functionality that undergoes reaction with a conserved cysteine residue present in EGFR (Cys797), heteroatom-linked pyrimidine 4-substituents, and presence of a pyrimidine 5-substituent], AZD9291 is architecturally unique. Among other differences, the electrophilic functionality resides on the pyrimidine C-2 substituent ring, the pyrimidine 4-substituent is C-linked and heterocyclic, and the pyrimidine 5-position is devoid of substitution.

In EGFR recombinant enzyme assays (Millipore), AZD9291 showed an apparent IC_{50} of 12 nmol/L against L858R and

1 nmol/L against L858R/T790M; these are called apparent because the amount of active enzyme changes over time and thus IC_{50} is time dependent for irreversible agents. The drug exhibited nearly 200 times greater potency against L858R/T790M than wild-type EGFR (Supplementary Table S1A), consistent with the design goal of a mutant EGFR-selective agent in comparison with early-generation TKIs. Subsequent murine *in vivo* studies revealed that AZD9291 was metabolized to produce at least two circulating metabolite species, AZ5104 and AZ7550. In biochemical assays, AZ7550 had a comparable potency and selectivity profile to the parent (Supplementary Table S1A). In contrast, although AZ5104 exhibited the same overall profile, it was more potent against mutant and wild-type EGFR forms, thus demonstrating a smaller selectivity margin compared with the parent (Supplementary Table S1A).

To explore a broader kinome selectivity profile, we tested AZD9291 and metabolites at 1 μ mol/L across approximately 280 other kinases available on a commercial biochemical kinome panel (Millipore). AZD9291 showed minimal off-target kinase activity, with only a limited number of additional kinases showing greater than 60% inhibition at 1 μ mol/L and moderate IC_{50} potencies such as ERBB2/4, ACK1, ALK, BLK, BRK, MLK1, and MNK2 (Supplementary Table S1B). The active metabolites displayed a similar secondary target profile as parent (Supplementary Table S1B). Given that AZD9291 makes a covalent bond with Cys797 in EGFR as described, we were specifically interested to explore potency in other kinases that have a cysteine residue in the analogous kinase domain position. Of the nine other kinases present within the human kinome with the analogous Cys797 to EGFR, AZD9291 showed significant activity only in a biochemical assay against ERBB2, ERBB4, and BLK (Supplementary Table S1B), supporting the overall high degree of selectivity that AZD9291 confers.

Like the T790M EGFR receptor, the insulin-like growth factor 1 receptor (IGF1R) and insulin receptor (IR) also have a methionine gatekeeper in their kinase domains. We considered it important to develop selectivity against these kinases to minimize potential dose-limiting toxicities related to hyperglycemia. Using a commercially available cellular IGF1R phosphorylation assay as a surrogate, AZD9291 and the metabolite AZ5104 did not exhibit significant activity toward this receptor family (Supplementary Table S1C). Moreover, a single oral dose of 200 mg/kg of AZD9291 in rats did not cause a significant change in blood glucose or insulin levels over a 24-hour period, consistent with lack of IGF1R activity (data not shown).

Finally, we evaluated cellular potency against HER2 (ERBB2), using three different cellular approaches: surrogate kinase assays involving expression of wild-type HER2 in HEK293 cells (Supplementary Fig. S2A), PC-9 cells (ex19del) engineered to overexpress HER2 (Supplementary Fig. S2B; ref. 13), and biochemical reconstitution studies in HEK293 cells involving intracellular domain constructs encoding L858R/T790M, wild-type EGFR, or wild-type HER2 (Supplementary Fig. S2C; ref. 37). Consistently, treatment of cells with AZD9291 inhibited phosphorylation of HER2 at moderate potency levels. However, consistent with its greater wild-type EGFR potency, the AZ5104 metabolite showed more potency than AZD9291 against phospho-HER2 (Supplementary Fig. S2A–S2C).

AZD9291 Potently and Selectively Targets Mutant EGFR Cell Lines *In Vitro*

We compared AZD9291 with other early-generation EGFR TKIs in EGFR phosphorylation and cell death (Sytox) assays using a number of tumor cell lines harboring either wild-type or different forms of mutant EGFR. Compared with other EGFR inhibitors of both first (gefitinib and erlotinib) and second (afatinib and dacomitinib) generation, AZD9291 demonstrated a unique third-generation TKI profile. AZD9291 showed similar potency to early-generation TKIs in inhibiting EGFR phosphorylation in EGFR cells harboring sensitizing EGFR mutants, including PC-9 (ex19del), H3255 (L858R), and H1650 (ex19del; Fig. 2A), with mean IC_{50} values ranging from 13 to 54 nmol/L for AZD9291. AZD9291 also potently inhibited phosphorylation of EGFR in T790M⁺ mutant cell lines [H1975 (L858R/T790M), PC-9VanR (ex19del/T790M); Fig. 2A], with mean IC_{50} potency less than 15 nmol/L. First-generation reversible TKIs were ineffective at inhibiting phosphorylation of EGFR^{T790M} (Fig. 2A). The second-generation irreversible TKIs, afatinib and dacomitinib, showed activity against EGFR^{T790M} *in vitro*, although this activity may not be achievable at exposures that can be reached in the clinic. AZD9291 was less potent at inhibiting phosphorylation of EGFR in wild-type cell lines (A431, LOVO, and NCI-H2073), with mean IC_{50} range of 480 to 1,865 nmol/L (Fig. 2A). This is in clear contrast with the early-generation TKIs, which all potently inhibited EGFR phosphorylation in wild-type lines with similar potency to sensitizing mutant EGFR (Fig. 2A). Similar results were found when phosphorylation of EGFR and downstream signaling was determined by immunoblot analysis of lysates from PC-9, H1975, LOVO, H1650, and H3255 lines (Fig. 2B). Consistently, results showed that AZD9291 more potently inhibited phospho-EGFR and downstream signaling substrates (phospho-AKT and phospho-ERK) in cells with mutant EGFR compared with wild-type (Fig. 2B), although H1650 cells retained higher phospho-AKT levels due to loss of PTEN (38).

As previously described, AZD9291 has active circulating metabolites, so we also profiled their activity against EGFR. Consistent with presented biochemical data, AZ7550 exhibited very similar potency and profile to AZD9291 against mutant and wild-type cell lines tested (Supplementary Table S1D), whereas AZ5104 harbored somewhat greater potency against ex19del (2 nmol/L in PC-9), T790M (2 nmol/L in H1975), and wild-type EGFR (33 nmol/L in LOVO) cell lines. Therefore, AZ5104 exhibited a reduced selectivity margin against wild-type EGFR when compared with AZD9291. However, taken together, these mechanistic data confirmed the third-generation TKI properties of AZD9291 compared with earlier generation agents: equivalent activity against sensitizing mutant EGFR, superior activity toward T790M, and increased selectivity margin against wild-type EGFR.

We then explored how the pharmacologic activity against mutant and wild-type EGFR signaling translated into cell proliferation effects using a Sytox live/dead cell phenotype endpoint. In line with the phosphorylation data, AZD9291 showed high levels of phenotype potency in both sensitizing mutant (mean IC_{50} of 8 nmol/L in PC-9) and T790M (mean IC_{50} of 11 and 40 nmol/L in H1975 and PC-9VanR, respectively) EGFR

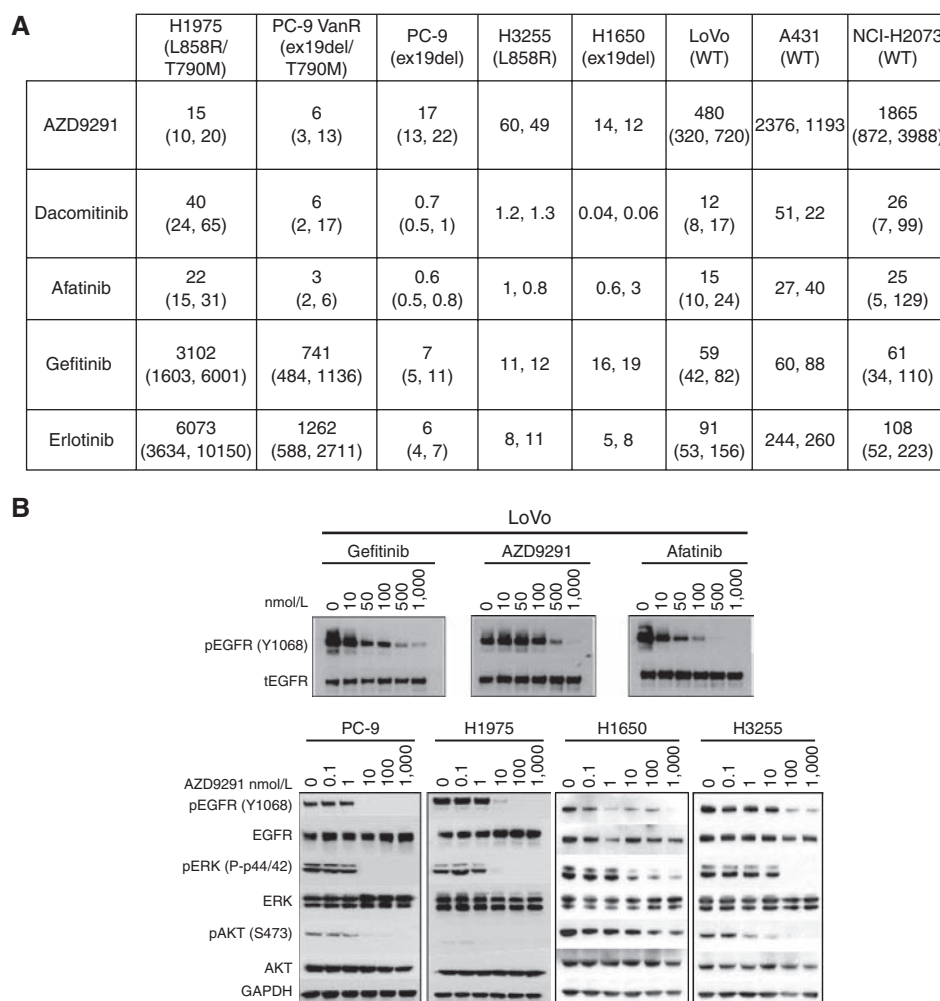


Figure 2. Effect of AZD9291 on EGFR phosphorylation *in vitro*. **A**, in comparison with early-generation TKIs, AZD9291 inhibits EGFR phosphorylation across cell lines harboring sensitizing (PC-9, H3255, and H1650) or T790M resistance (H1975 and PC-9VanR) mutations, while having less activity against wild-type EGFR phosphorylation (LoVo, A431, and H2073). Apparent geomean IC_{50} (nmol/L) values quantified in cell extracts after 2 hours of compound treatment using a phospho-EGFR ELISA from at least two separate experiments (expressed with 95% confidence intervals where $n > 3$, or individual IC_{50} values where $n = 2$). **B**, AZD9291 inhibits EGFR phosphorylation (p) and downstream signaling pathways across representative mutant EGFR lines (PC-9, H1975, H1650, and H3255), while having less activity against EGFR phosphorylation in the LoVo wild-type EGFR cell line compared with early-generation TKIs, after a 6-hour treatment. The data are representative of at least two separate experiments.

cell lines, while having much less activity toward wild-type EGFR (mean IC_{50} of 650 and 461 nmol/L in Calu3 and H2073, respectively; Fig. 3A). Again, this contrasted with second-generation TKIs afatinib and dacomitinib, which showed much less activity against T790M lines and were associated with much greater potency toward wild-type EGFR (Fig. 3A). To confirm these results, we determined the efficacy of AZD9291 in an independent laboratory against a panel of isogenic pairs of drug-sensitive/resistant EGFR-mutant lung cancer cell lines (31, 39). Parental EGFR^{wt} lines (PC-9, H3255, HCC827, HCC4006, and 11-18) were sensitive to AZD9291 as well as erlotinib, afatinib, and AZD8931 (a reversible equipotent inhibitor of EGFR, HER2, and HER3 signaling; ref. 40; Fig. 3B). However, only AZD9291 displayed low nanomolar activity against the lines harboring EGFR^{T790M} (H1975, HCC827/ER1, PC-9/BRc1, and H3255/XLR; Fig. 3B). Interestingly, AZD9291 was not effective against lines harboring non-T790M resistance, such as 11-18/ER (NRAS), HCC827/ER2 (*MET* amplification), and HCC4006/ER (EMT; ref. 17; Fig. 3B). In a separate large cell panel proliferation profiling study, AZD9291 was also poorly active *in vitro* ($IC_{50} \sim 1 \mu\text{mol/L}$) against both NSCLC NCI-H820 and EBC-1 cell lines that harbor *MET* amplification and mutant EGFR (data not shown). Consistent with phospho-EGFR data,

the metabolite AZS104 again demonstrated much greater potency across cell lines in a phenotypic assay, whereas AZ7550 was broadly similar, with the same overall profile maintained (Supplementary Table S1E).

Because of their low activity against EGFR^{T790M}, it has been suggested that treatment with early-generation TKIs can induce the growth selection of tumor cells harboring EGFR^{wt}/T790M, leading to TKI-resistant populations both preclinically and clinically (31). We therefore hypothesized that such resistance would not occur upon treatment with AZD9291, given its superior potency against T790M. Indeed, although chronic treatment with gefitinib or afatinib commonly caused acquired resistance in PC-9 cells *in vitro* through gain of T790M, acquired resistance to AZD9291 through T790M was not observed (Fig. 3C). Studies are ongoing to characterize the T790M-independent mechanisms of acquired resistance to AZD9291 (C. Eberlein and colleagues; manuscript in preparation).

Activity of AZD9291 against Rare EGFR and HER2 Mutants *In Vitro*

In addition to activity against the common activating/sensitizing EGFR mutants, we assessed the potency of AZD9291

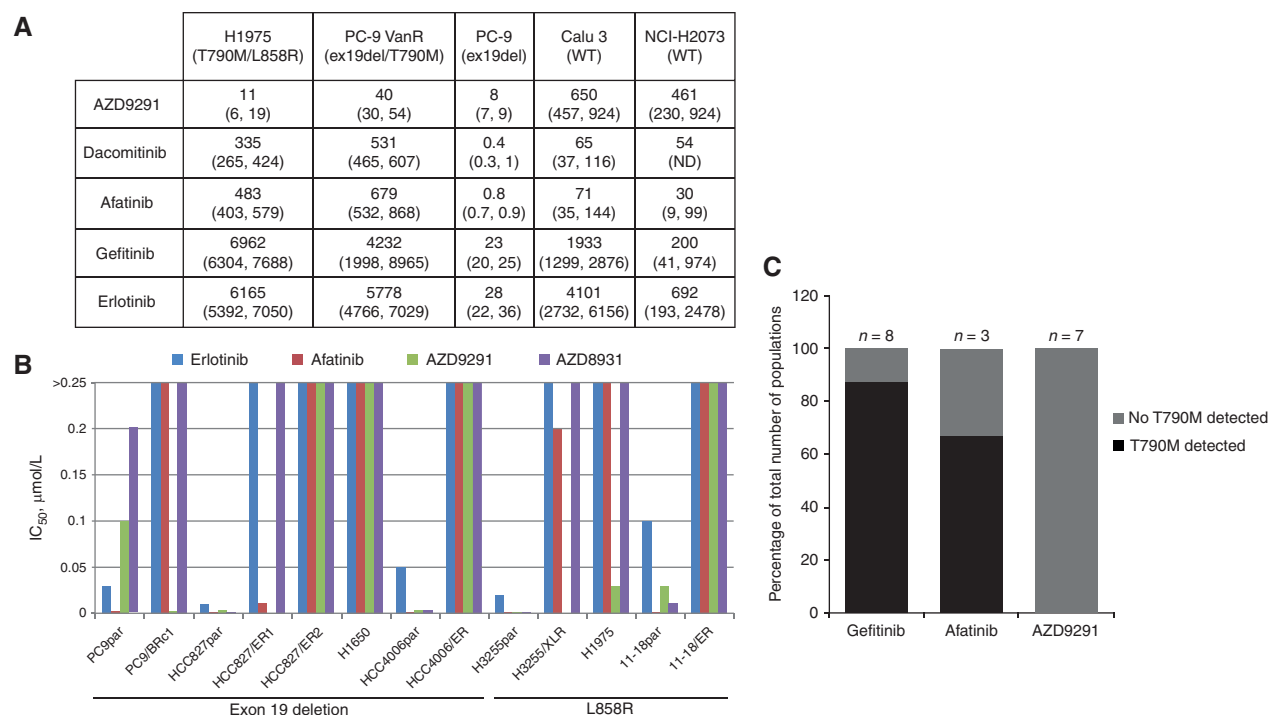


Figure 3. Additional characteristics of AZD9291 *in vitro*. **A**, AZD9291 demonstrates greater inhibition of viability against mutant EGFR cell lines compared with wild-type, as assessed using a Sytox Green live/dead assay measured after 3 days of treatment. The data represent the geomean IC_{50} nmol/L value from at least two separate experiments (expressed with 95% confidence intervals where $n > 3$). **B**, sensitivity of isogenic pairs of EGFR-mutant drug-sensitive and drug-resistant lung cancer cell lines (PC-9, ex19del; PC-9/BRc1, ex19del/T790M; HCC827, ex19del; HCC827/ER1, ex19del/T790M; HCC827/ER2, ex19del/MET amplification; H1650, ex19del/PTEN loss; HCC4006, ex19del; HCC4006/ER, EMT; H3255, L858R; H3255/XLR, L858R/T790M; H1975, L858R/T790M; 11-18, L858R; 11-18/ER, L858R/NRAS) to AZD9291, erlotinib, and afatinib. IC_{50} values (μ mol/L) were based on data obtained from growth inhibition assays. **C**, T790M mutation was detected in multiple independent populations of PC-9 cells with acquired resistance to gefitinib or afatinib, but not in populations resistant to AZD9291.

against other rarer EGFR mutants associated with sensitivity or resistance to first-generation EGFR TKIs (Supplementary Fig. S3). HEK293 cells were transfected with cDNAs encoding EGFR G719S, L861Q, an exon 20 insertion (H773-V774HVDup), an exon 19 insertion (I744-K745insKIPVAI), or an EGFR variant III (EGFRvIII; found in brain glioblastomas; ref. 41), and treated with increasing concentrations of either erlotinib, afatinib, AZD9291, the metabolite AZ5104, or AZD8931 for 6 hours. Immunoblotting was performed on corresponding lysates using antibodies against phospho-EGFR (Y1173) and total EGFR. All EGFR TKIs were effective against EGFR L861Q (consistent with kinase profiling data; Supplementary Table S1A), G719S, and the exon 19 insertion, although AZD9291 was somewhat less potent compared with the AZ5104 metabolite against these mutant EGFR forms (Supplementary Fig. S3A). None of the TKIs was effective against the exon 20 insertion mutation (Supplementary Fig. S3B). For the EGFRvIII mutant, AZD9291 demonstrated lower potency compared with afatinib and AZD8931. AZ5104, however, displayed a higher level of activity (Supplementary Fig. S3C). These data are consistent with the kinase activity of the vIII mutant being similar to that of wild-type EGFR.

We similarly explored activity against *HER2* mutations found in NSCLC. Compared with afatinib and AZ5104, AZD9291 exhibited moderate potency against H1781 cells, which harbor a VC insertion at G776 in exon 20 of *HER2*

(42), with an IC_{50} of 80 nmol/L (Supplementary Fig. S4A). However, AZD9291 was more effective at inhibiting growth of these cells than erlotinib. The effect of various TKIs on *HER2*-associated signaling in H1781 cells was consistent with these results (Supplementary Fig. S4B). Similar activity was observed in 293 cell transfectants harboring the most common *HER2* mutant in NSCLC (exon20 YVMA 776-779ins; ref. 43; Supplementary Fig. S4C). Thus, in patients, AZD9291 and its metabolite AZ5104 may also be able to target *HER2* in tumors, depending on the clinical exposures that are achieved.

AZD9291 Causes Profound and Sustained Regression in Mutant EGFR *In Vivo* Xenograft Models

AZD9291 demonstrated good bioavailability, was widely distributed in tissues, and had moderate clearance resulting in a half-life of around 3 hours after oral dosing in the mouse (Supplementary Fig. S5). The circulating active metabolites in plasma each had a similar half-life, and the total exposure levels (AUC) were approximately 68% and 33% compared with the parent compound for AZ7550 and AZ5104, respectively (Supplementary Fig. S5).

To explore *in vivo* activity of AZD9291, we administered the drug as monotherapy against various mutant EGFR xenografts representing clinical NSCLC settings. Once-daily

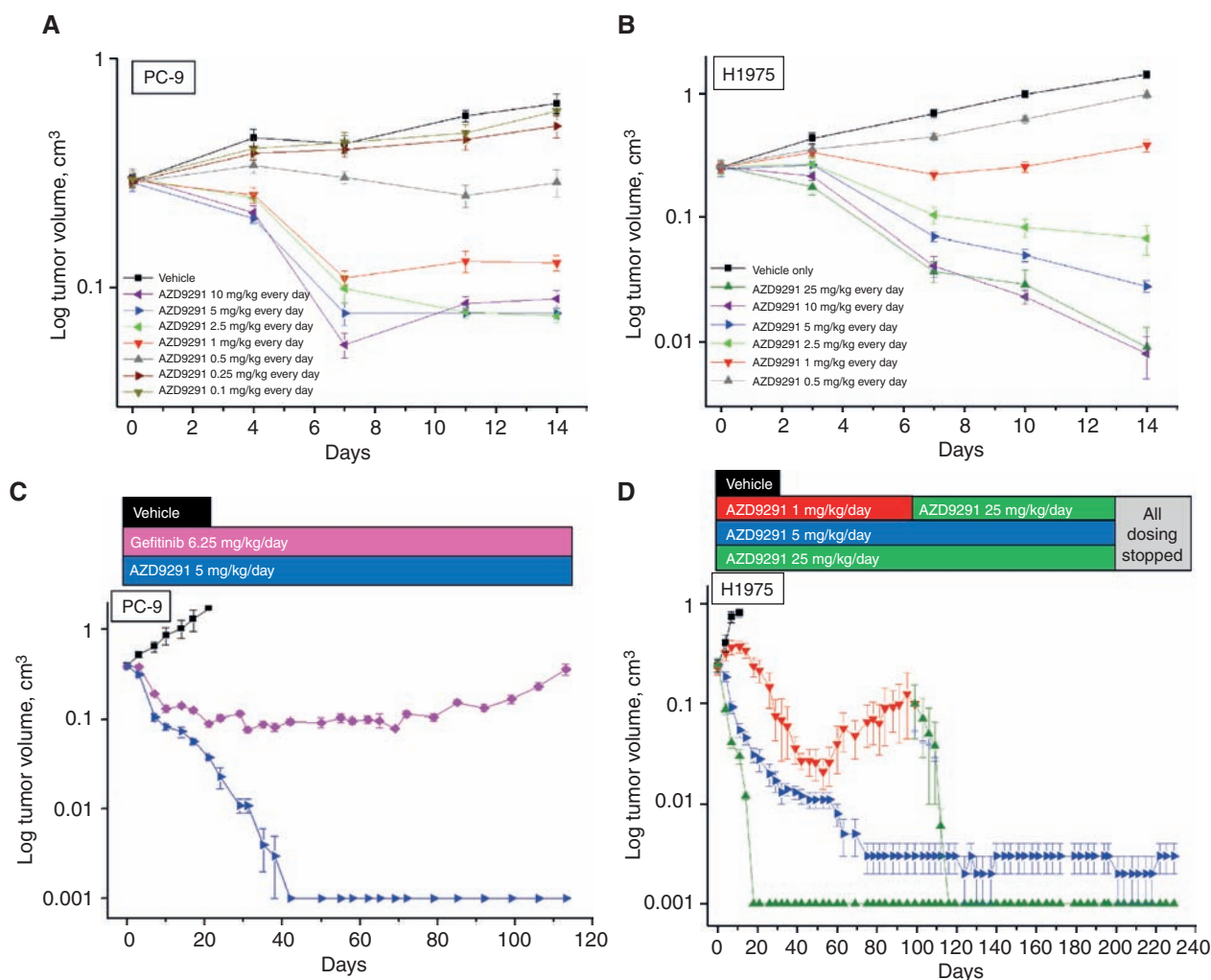


Figure 4. In vivo antitumor efficacy of AZD9291 in subcutaneous xenograft models of EGFR-TKI-sensitizing and T790M⁺ resistant lung cancer. **A**, PC-9 (ex19del) xenografts following 14 days of daily treatment ($n = 6$ or 8 animals depending on treatment group). **B**, H1975 (L858R/T790M) xenografts following 14 days of daily treatment ($n = 6$ or 8 animals depending on treatment group). **C**, PC-9 xenografts following chronic daily oral dosing of 5 mg/kg AZD9291 ($n = 8$) or 6.25 mg/kg gefitinib ($n = 11$). **D**, H1975 xenografts following chronic daily oral dosing of 1, 5, or 25 mg/kg AZD9291 ($n = 10$ or 12 animals depending on dose group). Data represents mean tumor volume, \pm SEM.

dosing of AZD9291 induced significant dose-dependent regression in both PC-9 (ex19del) and H1975 (L858R/T790M) tumor xenograft models, with tumor shrinkage observed at doses as low as 2.5 mg/kg/day in both models after 14 days (Fig. 4A and B). Similar tumor shrinkage was seen after administration of 5 mg/kg/day AZD9291 in H3255 (L858R; Supplementary Fig. S6A) and PC-9VanR (ex19 del/T790M; Supplementary Fig. S6B) xenografts after 14 days. These studies showed that AZD9291 can induce profound shrinkage at low doses against both EGFR drug-sensitizing and T790M⁺ resistant EGFR-mutant disease models.

We next explored the durability of tumor shrinkage. Chronic long-term daily oral dosing of AZD9291 resulted in complete and durable macroscopic responses of both PC-9 (Fig. 4C) and H1975 xenografts (Fig. 4D). For PC-9 cells, no visible tumors were evident following 40 daily doses with 5 mg/kg/day of AZD9291 in eight of eight tumors, and this complete response

was sustained out to 200 days, when the study was terminated (data not shown). As a comparison, gefitinib at 6.25 mg/kg/day, a clinically representative dose, induced less tumor regression, and tumors began to regrow after approximately 90 days. In H1975 xenografts, 5 mg/kg/day AZD9291 resulted in complete responses in 10 of 12 tumors. Regrowth was observed after approximately 50 days of treatment with 1 mg/kg/day, but an increased dose of 25 mg/kg/day AZD9291 reinduced tumor regression, possibly suggesting that regrowth was still driven by EGFR^{T790M}. No visible tumors were evident after 20 days of dosing of 25 mg/kg/day AZD9291 in the H1975 xenograft model. Moreover, the complete responses were maintained for the duration of the study period with no evidence of tumor progression during 200 days of treatment. No growth was observed for an additional 30 days after treatment was stopped. AZD9291 daily dosing was well tolerated in the animals, with minimal body weight loss (less than 5% of

starting body weight) even after dosing for 200 days [Supplementary Fig. S6C (PC-9) and S6D (H1975)]. Similar long-term dosing studies were performed in the H3255 model, with 5 mg/kg/day AZD9291 causing nonmeasurable tumors in all 8 dosed mice by day 53. In contrast, only 1 mouse treated with 6.25 mg/kg/day gefitinib achieved nonmeasurable tumor status (Supplementary Fig. S6A).

To explore comparative efficacy against wild-type EGFR, AZD9291 was tested in A431 xenografts. These cells are used as a model for wild-type EGFR activity, but they are highly dependent on amplified wild-type EGFR and, therefore, are unlikely to reflect normal tissue EGFR pharmacology/physiology (44). AZD9291 did induce some moderate tumor growth inhibition at 5 mg/kg/day (Supplementary Fig. S6E), suggesting that AZD9291 or associated metabolites are not entirely inactive against wild-type EGFR in this model. In contrast, this same 5 mg/kg/day dose level was sufficient to induce profound and sustained tumor shrinkage in both H1975 and PC-9 mutant EGFR tumor xenograft models (Fig. 4A and B), consistent with AZD9291 having a significant selectivity margin over wild-type EGFR.

AZD9291 Causes Profound and Sustained Regression in Mutant EGFR *In Vivo* Transgenic Tumor Models

We further examined tumor responses in previously generated mouse tumor models that develop lung adenocarcinomas driven by EGFR^{L858R} (45) or EGFR^{L858R + T790M} (46). These models use a tetracycline-inducible (tet-inducible) system, involving biransgenic animals. One transgene carries a tet transactivator in lung epithelia [i.e., Clara cell secretory protein–reverse tetracycline transactivator (CCSP-rtTA), herein referred to as “C” mice]. The two relevant strains are referred to as C/L858R and C/L+T, respectively. As expected, tumors harboring EGFR^{L858R} were sensitive to erlotinib, whereas tumors expressing EGFR^{L858R + T790M} were resistant (46). Here, we treated tumor-bearing mice with AZD9291 (5 mg/kg/day), afatinib (7.5 mg/kg/day), or vehicle control for 1 to 2 weeks. Within days of treatment, 5 of 5 C/L858R mice displayed nearly 80% reduction in tumor volume by MRI (see Methods and ref. 47) after therapy with both afatinib and AZD9291, whereas 5 of 5 mice treated with vehicle showed tumor growth (Figs. 5A, top and 5B). Upon histologic examination, only vehicle-treated mice showed viable tumor (Fig. 5B). In contrast, in C/L+T animals, only AZD9291 treatment induced significant tumor shrinkage (Figs. 5A, middle and bottom and 5C), whereas both vehicle- and afatinib-treated mice showed viable tumor (Fig. 5C). The difference in tumor responses was more pronounced after 2 weeks of treatment (Fig. 5A, bottom). Furthermore, preliminary data in a single mouse with a tumor driven by an ex19del-mutant alone (45) also responded rapidly to AZD9291 (Supplementary Fig. S7A). The metabolite, AZ5104 (5 mg/kg/day), was also effective in shrinking tumors in both C/L858R (Supplementary Fig. S7B and S7C) and C/L+T mice (Supplementary Fig. S7B and S7D).

Pharmacodynamic Confirmation of Target Inhibition by AZD9291

To confirm on-target and pathway activity of AZD9291, we examined tumor tissues from the H1975 xenograft and

L858R/T790M transgenic model after drug treatment. Mice bearing H1975 xenografts were given a single dose of AZD9291 (5 mg/kg) and tumors were harvested 1, 6, 16, 24, and 30 hours later. Sections from formalin-fixed paraffin-embedded tumors were then stained for the phosphorylated forms of EGFR (Tyr1173), ERK (Thr202/Tyr204), S6 (Ser235/236), and PRAS40 (Thr246). In the H1975 model, AZD9291 treatment strongly inhibited both phospho-EGFR and downstream signaling pathways after 6 hours (Fig. 6A). Although in mice, the pharmacokinetic half-life of AZD9291 is only approximately 3 hours, phospho-EGFR staining remained significantly diminished even after the 30-hour time point, consistent with its expected irreversible mode of action. Interestingly, although downstream signaling molecules similarly showed maximal inhibition after 6 hours, in contrast with phospho-EGFR, they displayed more transient inhibition (Fig. 6A).

In the transgenic model, we similarly observed target inhibition after 5 mg/kg dosing of AZD9291 via immunohistochemical staining of sections for phospho-EGFR and downstream markers (Fig. 6B) or immunoblotting of lysates (Fig. 6C) from treated tumors.

Proof-of-Principle Clinical Activity of AZD9291 in Patients with Acquired Resistance to EGFR TKIs

The mesylate salt of AZD9291 is currently in a first-in-human phase I dose-escalation clinical trial (AURA; NCT01802632; AstraZeneca) in patients with advanced EGFR^{m+} NSCLC who had disease progression following treatment with any EGFR TKI (including gefitinib or erlotinib). As proof of principle, here we present preliminary results of the first 2 patients in the study with confirmed radiographic responses (as per RECIST 1.1; ref. 48) treated at the lowest dose cohort (20 mg once daily; Fig. 7; ref. 49). Both patients' tumors harbored drug-sensitive EGFR mutations in addition to documented T790M mutations (according to local testing results). Consistent with AZD9291 being less active against wild-type EGFR, in these two cases there were no rash events and only one reported CTCAE grade 1 diarrhea. Preliminary clinical pharmacokinetic analysis indicates that AZD9291, AZ5104, and AZ7550 have a half-life of at least 50 hours, longer than would be predicted from the preclinical data, which results in a desirable flat pharmacokinetic profile after multiple once-daily dosing (Fig. 7A). Further phase I clinical data for this study will be submitted for publication at a later date.

The first patient was a 57-year-old East Asian female from South Korea diagnosed with stage IV EGFR-mutant (ex19del) NSCLC in May 2011. The patient had disease progression following two cycles of gemcitabine plus carboplatin combination chemotherapy. The patient next had a partial response on gefitinib before developing disease progression after 10 months. She then had stable disease with four cycles of pemetrexed followed by four cycles of paclitaxel plus carboplatin with a best response of partial response before progressing immediately before study. Analysis of tumor tissue, from a biopsy taken immediately before AZD9291 study entry, using direct dideoxynucleotide-based sequencing, revealed the presence of a T790M mutation (data not shown). Tumor shrinkage on AZD9291 was 39.7% at scan 1, 48.3% by scan 2 (Fig. 7B), remained at 48.3% at both scans 3 and 4, and was 51.7% at scan 5 (data not shown).

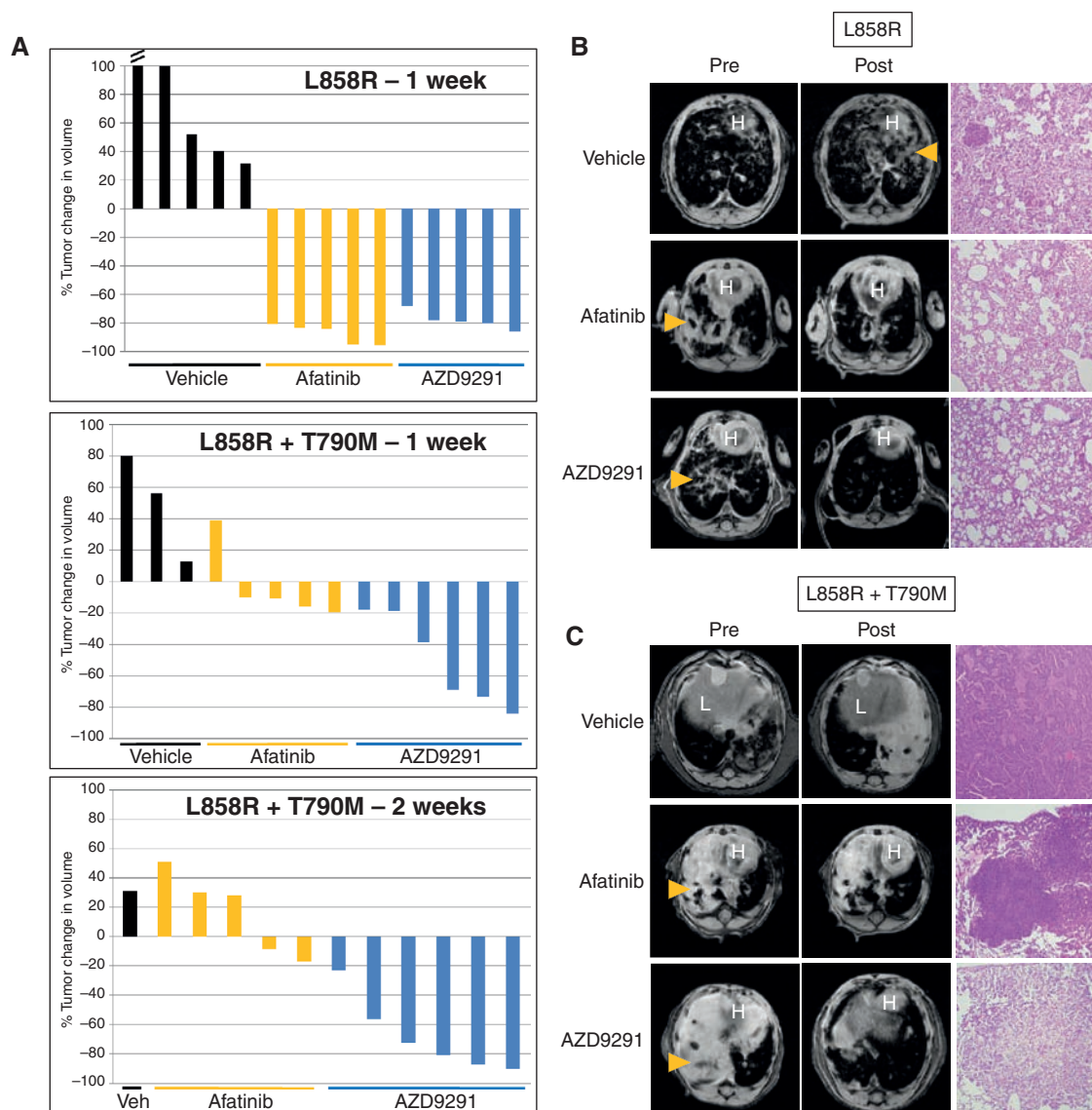


Figure 5. AZD9291 induces significant and sustained tumor regression in transgenic models of EGFR-TKI-sensitizing (C/L858R) and T790M⁺ resistant (C/L+T) lung cancer. **A**, percent change in radiographic tumor volume from baseline by treatment of individual lung tumor-bearing C/L858R (top) and C/L+T (middle, bottom) animals with vehicle, afatinib (7.5 mg/kg/day), or AZD9291 (5 mg/kg/day). **B** and **C**, representative MRI images and hematoxylin and eosin (H&E) staining (original magnification, $\times 40$) of lungs from tumor-bearing animals (B, C/L858R and C, C/L+T) pre- and posttreatment with vehicle, afatinib, or AZD9291 for 1 week. H, heart; L, liver; arrow, tumor.

The second patient was a 57-year-old white female never-smoker from England diagnosed with stage IV lung adenocarcinoma in December 2010. Analysis of tumor tissue obtained at diagnosis in a local molecular pathology laboratory using the Qiagen EGFR RQ PCR test revealed evidence of exon 19 deletion and T790M mutations (data not shown). The patient was treated with first-line gefitinib, achieving a partial response before eventual progressive disease 14 months later, suggesting that the T790M mutation was present at only a low allele frequency. Rebiopsy before starting AZD9291 was not performed. At the cycle 1 day 15 assessment on AZD9291, the patient reported full resolution of preexisting persistent nocturnal cough. Tumor shrinkage was 38%

at scan 1, 39.3% at scan 2, 56.7% by scan 3 (Fig. 7C), 62% by scan 4, and 59.3% by scan 5 (data not shown). By cycle 7 day 1, the patient reported significant improvement in preexisting hair and eyelash abnormalities, which had developed during the immediately prior gefitinib therapy. Because this patient received AZD9291 after developing acquired resistance while on continuous gefitinib (after initial >6 months duration of partial response) with no intervening treatment, strict Jackman clinical criteria for acquired resistance were fulfilled (50). No significant aberration of blood glucose levels was noted in either patient during the study. Both patients had a duration of response of approximately 9 months and were progression free on 20 mg/day AZD9291 for approximately 11 months,

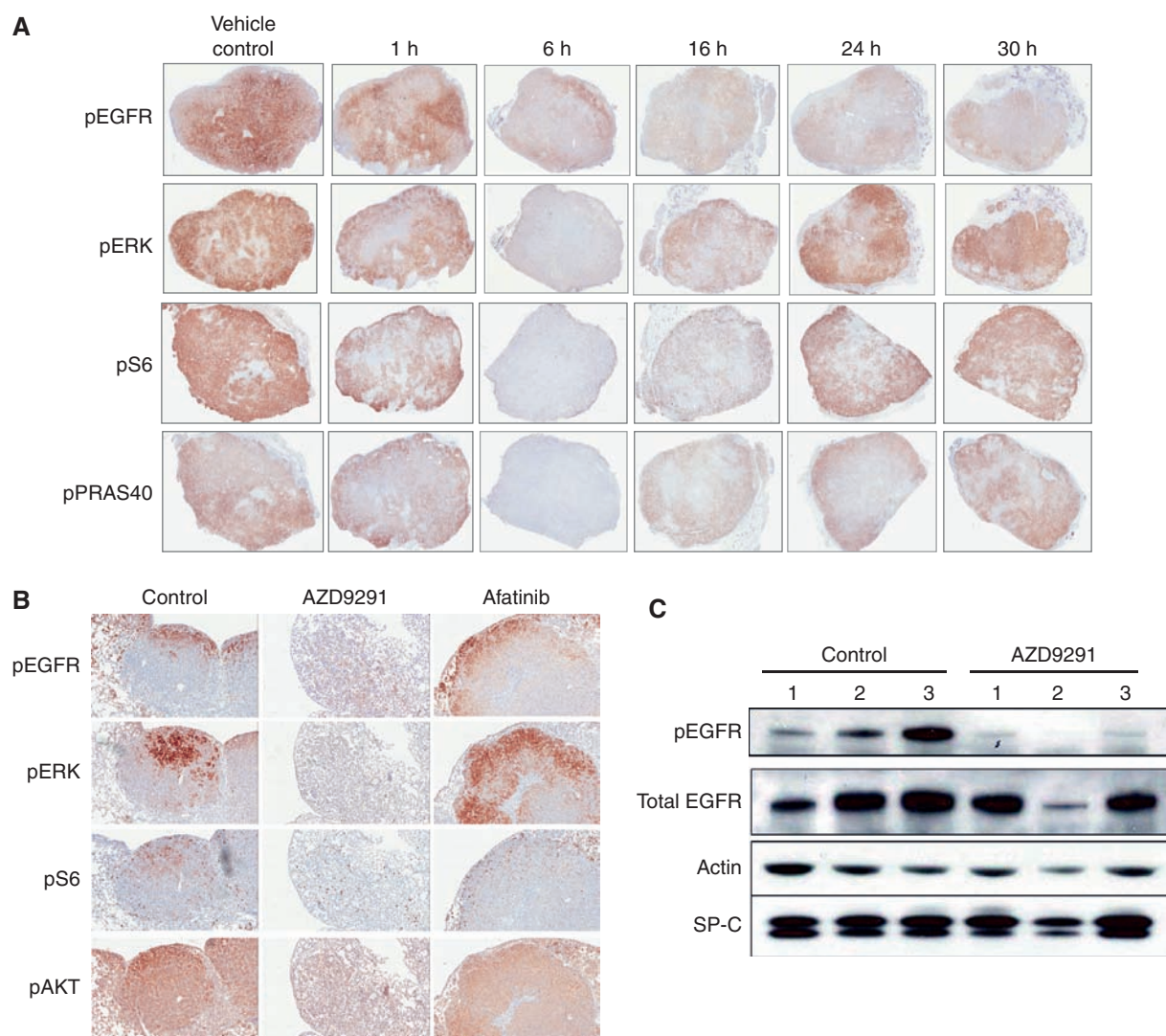


Figure 6. AZD9291 inhibits EGFR phosphorylation and downstream signaling in murine models of EGFR^{T790M}-resistant lung cancer. **A**, subcutaneous H1975 (L858R/T790M) xenografts, treated with a single 5 mg/kg dose of AZD9291 for the indicated times, were examined for phospho (p) EGFR, ERK, S6, and PRAS40 status by immunohistochemistry. Representative images were taken from scans at $\times 20$ magnification and then size adjusted to fill the screen. **B**, lungs from representative transgenic mice treated with control, AZD9291, or afatinib were harvested 6 hours after dose administration. Formalin-fixed paraffin-embedded sections were stained with the indicated antibodies. Representative images were taken from Aperio scans at $\times 100$ magnification. **C**, lungs were harvested from either untreated tumor-bearing transgenic mice (as confirmed by MRI; control) or from tumor-bearing mice 8 hours after a single treatment with AZD9291 5 mg/kg. Corresponding lysates from individual animals were immunoblotted with the indicated antibodies. Anti-SP-C (surfactant protein C) antibody was used as a surrogate marker for tumor burden, as tumors express the protein.

until disease progression by RECIST 1.1. Both patients continue to receive AZD9291 treatment on study as per protocol, as they continue to derive clinical benefit according to their treating physicians.

DISCUSSION

Mutations in *EGFR* occur in 10% to 35% of NSCLCs and confer sensitivity to the EGFR TKIs erlotinib, gefitinib, and afatinib (6). In randomized studies, the median overall survival of patients with *EGFR*-mutant lung cancer receiving first-line EGFR TKIs is approximately 19 to 36 months, whereas median progression-free survival is about 9 to 14 months.

In more than half of patients, tumor cells at the time of progression harbor a second-site T790M mutation, which confers resistance to these EGFR TKIs (23). No specific treatments for patients with acquired resistance to current EGFR TKIs have yet been approved.

We describe here the identification, characterization, and early clinical development of AZD9291, a novel oral, irreversible, third-generation TKI with a distinct profile from gefitinib, erlotinib, afatinib, and dacomitinib. Notably, AZD9291 has a distinct chemical structure from the other third-generation TKIs, WZ4002 (34) and CO-1686 (35). Biochemical profiling together with *in vitro* cellular phosphorylation and phenotype studies have collectively shown that

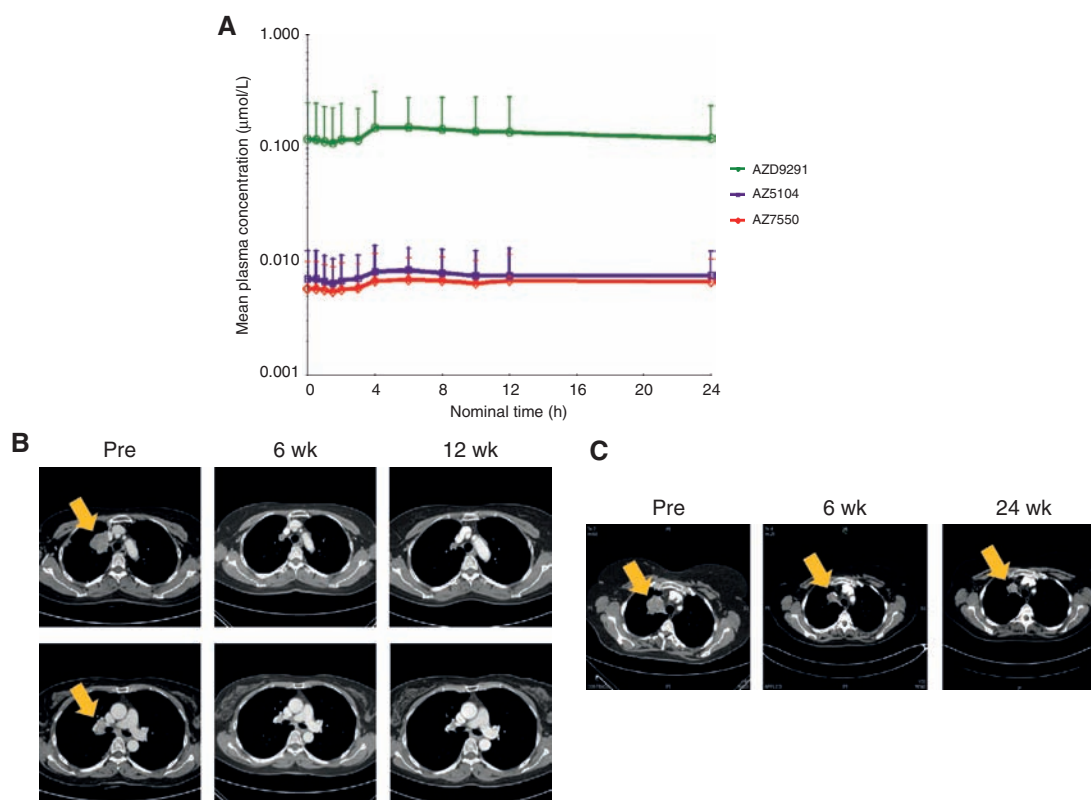


Figure 7. Proof-of-concept clinical studies validating AZD9291 as a mutant-selective EGFR kinase T790M inhibitor. **A**, preliminary pharmacokinetic profile showing mean (\pm SD) total plasma levels of AZD9291, AZ5104, and AZ7550 versus time from a cohort of 6 patients with advanced NSCLC after a single dose of AZD9291 mesylate salt, followed by a 7-day washout and then 8 days of once-daily 20 mg oral dosing in AURA phase I study (NCT01802632). **B** and **C**, serial computed tomography scans of the chest from patients before and after treatment with AZD9291 in a phase I trial. **B**, images from a 57-year-old Korean female patient diagnosed with stage IV NSCLC in May 2011. See the main text for details. **C**, images from a 57-year-old British female never-smoker diagnosed with stage IV lung adenocarcinoma in December 2010. The patient was previously treated with first-line gefitinib for 14 months, achieving a partial response before eventually developing progressive disease. See the main text for details.

AZD9291 is highly potent against EGFR^m and T790M⁺ resistant EGFR mutants with a wide margin of selectivity against wild-type EGFR activity and exhibits a high degree of selectivity against other kinases outside the EGFR family. Moreover, the profound antitumor activity of AZD9291 across xenograft and transgenic mutant T790M EGFR disease models *in vivo* suggests the potential to target T790M tumors following progression on early-generation TKIs.

Before identification of “third-generation” EGFR TKIs, the most promising targeted regimen in patients with acquired resistance had been the combination of afatinib plus cetuximab, which induced a 29% response rate and median progression-free survival of 4.7 months in a heavily pretreated cohort (33) with a significant degree of skin and gastrointestinal (diarrhea) toxicity. In the phase I trial of AZD9291 in patients with EGFR^m NSCLC that had progressed on earlier-generation TKIs, evidence of efficacy has been seen at all doses studied so far, with AZD9291-induced partial radiographic responses in patients whose tumors were known to harbor T790M, from the first dose cohort onwards (49, 51). Rash and diarrhea were mostly mild and reported in only a minority of patients, consistent with low activity against wild-type EGFR. Out of the two confirmed partial responses

described in this article, in addition to both patients’ tumors harboring the T790M mutations (according to local tests), one patient’s disease fits strict Jackman criteria for acquired resistance (50), receiving the drug directly after prolonged response and progression on gefitinib. Thus, based on the above, AZD9291 has already demonstrated proof-of-principle clinical activity in patients with acquired resistance for whom there are no approved targeted therapies. Similarly, results from a phase I trial with CO-1686 have also shown evidence of efficacy in TKI-resistant tumors harboring T790M (52, 53), providing further proof of principle for potential use of “third-generation” TKIs in this setting. A surprising finding in the afatinib plus cetuximab study was that tumors with undetectable levels of T790M also displayed tumor shrinkage, suggesting that a T790M-independent but EGFR-dependent pathway of resistance exists. The current phase I study of AZD9291 will test whether the drug is effective in both T790M-positive and T790M-negative cohorts, through planned dose-expansion cohorts. Full phase I data will be presented at completion of study.

The existence of cell populations harboring T790M within a proportion of TKI-naïve EGFR^m tumors has been reported, although the prevalence depends on the diagnostic assay

being used. Studies using more conventional diagnostic assays have reported detection in about 2% of TKI-naïve tumors (54). Recently, groups using more sensitive technologies have reported higher detection rates ranging from 40% to 60% (55), although it remains unclear whether all these observations are real or analytical artifacts (56). However, overall, the data support the hypothesis that T790M clones may preexist in a proportion of EGFR⁺ tumors before TKI treatment. In addition to T790M, AZD9291 also potently inhibits sensitizing mutant EGFR across *in vitro* and *in vivo* disease models at similar potencies to T790M⁺ mutant EGFR. Therefore, taken together, this supports the hypothesis that AZD9291 could also offer an attractive treatment option in EGFR⁺ TKI-naïve patients, through targeting both sensitizing and T790M tumor cell populations that coexist in a proportion of tumors, which may then lead to delayed disease progression and ultimately increased survival benefit. However, it remains to be determined what the optimal sequencing of EGFR TKIs will be and whether maximum benefit to most patients will be achieved through using AZD9291 after TKI progression or earlier in the treatment pathway.

Patients harboring EGFR⁺ tumors often progress during TKI treatment due to growth of secondary brain metastases (57). Although there are reports of TKIs providing benefit in treatment of EGFR⁺ brain metastases, current TKIs are believed to have generally poor properties for penetrating across the blood-brain barrier (BBB), and, thus, their activity will be variable and influenced by such factors as dose, level of BBB disruption, and efflux transporter expression across individuals. Therefore, there is also a need for EGFR TKIs with improved brain penetrance. Quantitative whole-body autoradiography (QWBA) studies in rat brain with [¹⁴C]AZD9291 have indicated that AZD9291 had a brain-to-blood ratio of up to 2 over the first 24 hours, suggesting the potential of AZD9291 to penetrate the brain (data not shown). This is in contrast with [¹⁴C]gefitinib, which had a maximum brain-to-blood ratio of only 0.2 (58). Although further preclinical studies are required to explore the translatable potential of AZD9291 to target brain metastases, together with future clinical studies, the preliminary data look promising in this area.

Despite the potential of AZD9291 to prevent resistance via T790M, tumors are likely to engage alternative escape mechanisms. If TKIs such as AZD9291 become a prominent feature in the treatment of EGFR⁺ disease across multiple lines of therapy, it will be critical for future preclinical and clinical research to identify the most prevalent resistance mechanisms. Consistent with its pharmacologic profile, we have not observed acquired resistance to AZD9291 *in vitro* due to emergence of T790M. It is also interesting to note that we have not yet seen resistance to AZD9291 due to direct mutation of cysteine 797 (data not shown), which would render the receptor refractory to irreversible agents; in an analogous manner T790M prevents inhibition by early-generation drugs. Therefore, non-EGFR-related resistance mechanisms may become more dominant for agents such as AZD9291. Indeed, preclinical reports have suggested that “third-generation” agents can induce switching to multiple signaling mechanisms that bypass EGFR dependency such as ERK and AKT pathways

(35, 59, 60). Because AZD9291 is structurally distinct, it will be critical to understand which resistance mechanisms are induced through treatment with AZD9291 and whether different “third-generation” TKIs engage common escape mechanisms. Furthermore, identification of molecular mechanisms of resistance will support the investigation of strategies to combine additional novel targeted therapies with AZD9291 as a foundation EGFR TKI partner, to achieve potentially greater clinical benefit.

AZD9291 and its active circulating metabolite AZ5104 display similar and minimal off-target activity against other non-HER family kinases, but *in vitro* data suggest the potential to target both HER2 and HER4 kinase activity. This property may be important, as *HER2* amplification may mediate acquired resistance to EGFR TKI in some cases (13). AZD9291 and AZ5104 also seem to be effective against other rare drug-sensitive EGFR mutants and potentially lung cancer-associated HER2 mutants, but like other EGFR TKIs are not potent against an *EGFR* exon 20 insertion. Further preclinical and clinical studies are required to understand the potential utility of AZD9291 in these additional molecular phenotypes.

Earlier-generation EGFR TKIs have revolutionized the treatment of EGFR⁺ NSCLC and have demonstrated the power of precision medicine in genetically defined tumors. However, toxicities related to wild-type EGFR and the emergence of resistance mechanisms have limited the effectiveness of these drugs. Third-generation EGFR TKI agents such as AZD9291 have the potential to overcome these limitations and improve markedly the treatment options for patients who have progressed on TKI treatment due to T790M. Evaluation of AZD9291 in the first-line setting in patients with EGFR⁺ tumors should also be considered on the basis of AZD9291's third-generation EGFR TKI profile. Moreover, if AZD9291 is confirmed to have a mild side-effect profile together with its clinical efficacy and mechanistic hypothesis, this raises the option for investigation as a foundation EGFR TKI for combinations with other therapies to provide further treatment options for patients.

METHODS

Modeling the Binding Mode of AZD9291

A published structure of the EGFR^{T790M} mutant (pdb code 3IKA; ref. 34) was used for the modeling of potential binding modes of AZD9291. Crystal structures were prepared using the protein preparation wizard in Maestro (Schrödinger Release 2013-1), which optimizes hydrogen placements. The active site was defined by using the bound ligand, and the covalent docking protocol was used to model potential binding modes. These were ranked using the assigned scores and manually inspected for the retention of the key hinge interactions to the hinge region residue M793.

Cell Lines

All AZ cell lines were tested and authenticated by short-tandem repeat (STR) analysis. PC-9 cells were obtained in November 2011 from Akiko Hiraide at AstraZeneca Japan and last STR tested in May 2013. NCI-H1975 (H1975; CRL-5908; obtained 2004 and last STR tested November 2012), Calu-3 (HTB-55; obtained 2010 and last STR tested June 2013), NCI-H1650 (H1650; CRL-5883; obtained 2004 and last STR tested September 2011), and NCI-H2073 (H2073;

CRL-5918; obtained 2007 and last STR tested November 2012) cells were obtained from the ATCC. LoVo cell line (CCL-229) was obtained from the European Collection of Animal Cell Cultures (ECACC) in 1995 and last STR tested in January 2013. PC-9 vandetanib-resistant cells (PC-9VanR) were obtained in 2010 from Dr. Kiura at Okayama University (Okayama, Japan) and last STR tested in September 2011. The A431 cell line was obtained in 2004 from Prof. Mike Waterfield at London Research Institute (London, United Kingdom), and STR tested in May 2012. All other cell lines were available in the Pao laboratory and have been used as reagents in the Pao laboratory since 2005. Pao laboratory cell lines were genotyped multiple times to confirm the presence of known *EGFR* mutations by standard Sanger sequencing to ensure the accuracy of experiments. Cells were cultured in standard RPMI-1640 media (Corning) supplemented with 10% heat-inactivated fetal bovine serum (Atlanta Biologicals), 2 mmol/L L-glutamine (Corning), and 1% penicillin/streptomycin (Corning) and grown in a humidified incubator with 5% CO₂ at 37°C. Resistant cells were maintained under constant TKI selection before use in experiments.

In Vitro EGFR Phosphorylation Assays

Cells were treated for 2 hours with a dose-response of each drug. Wild-type cells were stimulated for 10 minutes with 25 ng/mL of EGF before lysis. Level of EGFR phosphorylation was quantified in cell extracts using a modified R&D Systems DuoSet Human phospho-EGFR ELISA (36).

In Vitro Cell Phenotype Assays

Cellular Sytox proliferation assays were performed as described (36), and Origin software was used to interpolate IC₅₀ values. Growth-inhibition assays were performed using CellTiter Blue Reagent (Promega; G8081) as described (13), and IC₅₀ values were calculated using Excel (Microsoft).

Generation of EGFR Inhibitor-Resistant Cell Populations

PC-9 cells were seeded into T75 flasks (5×10^5 cells per flask) in RPMI-1640 growth media and incubated at 37°C in 5% CO₂. The following day, the media were replaced with media supplemented with a concentration of EGFR inhibitor equal to the EC₅₀ concentration predetermined in PC-9 cells. Media changes were carried out every 2 to 3 days, and resistant clones were allowed to grow to 80% confluency before the cells were trypsinized and reseeded at the original seeding density in media containing twice the concentration of EGFR inhibitor. Dose escalations were continued until a final concentration of 1.5 μ mol/L gefitinib, 1.5 μ mol/L afatinib, 1.5 μ mol/L WZ4002, or 160 nmol/L AZD9291 was achieved.

Expression Vectors and Transfections

The indicated EGFR cDNAs were cloned into the pcDNA3.1(-) expression vector and altered using site-directed mutagenesis as described (5). All cDNAs were resequenced to verify that no additional codon-changing mutations were present. pCDH-puro-EGFRvIII lacking exons 2 to 7 in *EGFR* (a kind gift from Dr. Jialiang Wang, Vanderbilt University, Nashville, TN) was constructed by subcloning the EGFRvIII fragment from MSCV-XZ066-EGFRvIII (Addgene; Plasmid# 20737; <http://www.addgene.org/20737/>) into the expression vector pCDH-CMV-MCS-EF1-Puro. pBabe-HER2YVMA-puro (a kind gift from Carlos Arteaga, Vanderbilt University, Nashville, TN) encoded HER2 with an in-frame YVMA insertion at residue 776 (43). All plasmids were transfected into 293 cells as described (5).

Immunoblotting

Cells were washed on ice with cold PBS before the addition of RIPA buffer (150 mmol/L Tris-HCl, pH 7.5, 150 mmol/L NaCl, 1%

NP-40 substitute, 0.1% SDS) supplemented with protease inhibitor cocktail (Roche), 40 mmol/L sodium fluoride, 1 mmol/L sodium orthovanadate, and 1 μ mol/L okadaic acid. After scraping, lysates were transferred to microcentrifuge tubes and shaken at 4°C for 20 minutes before 10-minute centrifugation and protein quantification with Bradford Reagent (Bio-Rad). Equal protein amounts were loaded for SDS-PAGE using 4% to 12% gradient or 10% Bis-Tris precast gels (Novex Life Technologies), followed by transfer to polyvinylidene difluoride membranes using the iBlot dry transfer system (Novex Life Technologies). After blocking in 5% BSA-TBST or milk-TBST, membranes were blotted with total EGFR (BD Biosciences; #610017), phospho-EGFR (Tyr1068, R&D Systems; MAB3570 or Tyr1173, Santa Cruz Technologies, Inc.; sc-12351), total AKT (Cell Signaling Technology; 9272S), phospho-AKT (Ser473; Cell Signaling Technology; 9271L), total ERK (Cell Signaling Technology; 9102L), phospho-ERK (Thr202/Tyr204; Cell Signaling Technology; 9101L), prosurfactant protein C (Abcam; ab90716), or actin (Sigma; A2066) followed by horseradish peroxidase (HRP)-conjugated secondary antibodies (Cell Signaling Technology; 7074 or 7076). Signals were detected with Western Lightening Plus detection reagents (PerkinElmer; NEL10500NEA).

Molecular Genotyping

AZD9291-resistant cells were assessed for EGFR^{T790M} and other recurrent lung-associated mutations using an established assay (61).

Xenograft Studies

All studies involving animals in the United Kingdom were conducted in accordance with U.K. Home Office legislation, the Animal Scientific Procedures Act 1986 (ASPA), and AstraZeneca Global Bioethics policy. All experimental work is outlined in project license 40/3483, which has gone through the AstraZeneca Ethical Review Process. NCI-H1975 and A431 cells for *in vivo* implant were cultured in DMEM (Invitrogen) supplemented with 10% v/v fetal calf serum (Sigma-Aldrich) and 1% v/v L-glutamine (Invitrogen). PC-9 cells were cultured in RPMI-1640 (Invitrogen) supplemented with 10% v/v fetal calf serum, 1% v/v L-glutamine, and 10% v/v M1 supplement (EGG Technologies). All cell lines were then cultured in a humidified incubator with 7.5% CO₂ at 37°C. Cells were detached using 0.05% trypsin (Invitrogen) and resuspended for implant in serum-free media. Approximately 5×10^6 cells were implanted subcutaneously in a total volume of 0.1 mL/mouse for PC-9 and NCI-H1975, and 1×10^7 cells were implanted subcutaneously for A431. Both PC-9 and A431 cells were implanted in 50% Matrigel. PC-9 xenografts were established in female SCID mice and NCI-H1975 and A431 were established in female nude mice. All mice were older than 6 weeks at the time of cell implant. Tumor growth was monitored twice weekly by bilateral caliper measurements, tumor volume was calculated, and mice were randomized into vehicle or treatment groups with approximate mean start size of 0.2 to 0.4 cm³. Randomization for animal studies was based on initial tumor volumes to ensure equal distribution across groups. A power analysis was performed whereby group sizes were calculated to enable statistically robust detection of tumor growth inhibition. Mice were dosed once daily by oral gavage for the duration of the treatment period. Tumor growth inhibition from start of treatment was assessed by comparison of the mean change in tumor volume for the control and treated groups. Statistical significance was evaluated using a one-tailed Student *t* test.

For pharmacodynamic studies, mice were randomized at a mean tumor volume of approximately 0.5 to 0.8 cm³ using the same randomization criteria as the tumor growth inhibition studies. Mice were then treated orally with a single bolus dose of either vehicle or AZD9291. Tumors were excised at specific time points after dosing and fixed in 10% buffered formalin. Immunohistochemical analysis was performed on formalin-fixed, paraffin-embedded tissue sections

staining for phosphorylated EGFR (Tyr1173) and phosphorylated ERK (p44/42 Thr202/Tyr204).

Transgenic Mouse Studies

All animals were kept in pathogen-free housing under guidelines approved by the Vanderbilt University Medical Center Institutional Animal Care and Use Committee. The generation of EGFR^{L858R} (45) and EGFR^{L858R+T790M} mice (male and female) was previously described (46). Doxycycline was administered by feeding mice (~3-week-old) with doxycycline-impregnated food pellets (625 ppm; Harlan-Teklad), and mice were treated for about 3 months, during which time tumors developed. Afatinib and AZD9291 were suspended in 1% Polysorbate 80 and administered via oral gavage once daily at the doses of 7.5 and 5 mg/kg, respectively. Mice were imaged weekly at the Vanderbilt University Institute of Imaging Science. For immunoblot analysis, mice were treated for 8 hours with drug as described before dissection and flash freezing of the lungs. Lungs were pulverized in liquid nitrogen before lysis as described above.

MRI

All procedures were approved by Vanderbilt's Institutional Animal Care and Usage Committee. Mice were anesthetized via inhalation of 2%/98% isoflurane/oxygen and maintained under anesthesia throughout the course of the experiment. Animals were secured in a prone position in a 38-mm inner diameter radiofrequency (RF) coil and placed in a Varian 7T horizontal bore imaging system (Varian, Inc.) for data collection. A constant body temperature of 37°C was maintained using heated air flow. Before treatment, mice were scanned at least twice to confirm the presence of growing lung nodules and to avoid treating false-positive animals.

Multislice T1-weighted gradient echo images were collected in all three imaging planes (axial, sagittal, and coronal) for the localization of the lungs [repetition time (TR) = 100 ms, echo time (TE) = 5 ms, slice thickness = 1 mm, 40 mm × 40 mm field of view (FOV), approximately 15–20 slices]. Following the initial scout imaging, respiratory triggered, segmented fast low angle shot (FLASH) images were collected in both the axial and coronal planes with TR/TE = 850/2.8 ms, flip angle = 15°, number of slices = 22, slice thickness = 0.7 mm with a 0.2-mm gap between slices, and number of acquisitions = 16. For the axial images, the FOV was 23.04 mm × 23.04 mm, with a matrix size of 256 × 256, resulting in an in-plane resolution of 90 μm. For the coronal orientation, the FOV was 30.72 mm × 23.04 mm, with a data matrix of 256 × 256, resulting in an in-plane resolution of 120 × 90 μm.

Following image acquisition, lung tumor volume measurements were performed using Matlab 2012a (The MathWorks, Inc.). A region of interest (ROI) was manually drawn around the lungs for each slice, excluding the heart, and a signal intensity threshold of 25 times the noise level (defined as the standard deviation of signal intensities in a region of the image background) was used to segment voxels within that ROI as positive for tumor. Total lung tumor volume was then calculated by multiplying the tumor area within the segmented region by 0.09 cm (the distance between each MRI slice).

Immunohistochemistry

Sections (4 μm) were deparaffinized with xylene and rehydrated through graded alcohols into water. Antigen retrieval was carried out in a Milestone RHS microwave rapid histoprocessor for 10 minutes at 110°C in pH9 buffer, Dako S2367 (for phospho-EGFR and phospho-AKT) and pH 6 citrate buffer, Dako S1699 (for phospho-Erk and phospho-S6). Tissues were placed on a Lab Vision Autostainer, endogenous peroxidase was blocked with 3% H₂O₂ for 10 minutes, followed by washing twice in TBS/0.05% Tween. Serum-free protein block (Dako; X0909) was applied for 15 minutes. Slides were then incubated with the primary antibodies at room temperature, phospho-EGFR Tyr1173 (Cell Signaling Technology; code 4407) at

a 1:200 dilution, phospho-ERK (p44/42 Thr202/Tyr204; Cell Signaling Technology; code 4376) at 1:100, phospho-S6 (Ser 235/236) CST #4857 at 1:150, phospho-PRAS40 (pThr246; Cell Signaling Technology; code #2997) at 1:200, and phospho-AKT308 CST #2965 at 1:100 dilution. After washing twice, sections were incubated for 30 minutes with Rabbit EnVision polymer detection system (Dako; K4003), washed twice, and then developed in liquid 3,3'-diaminobenzidine (DAB) for 10 minutes. Sections were then counterstained with Mayer's hematoxylin, dehydrated, cleared, and mounted with coverslips.

Patients

All patients were treated on trial NCT01802632 with written informed consent and approval from appropriate Institutional Review Boards (for the 2 patients disclosed in this article, the Ethics committees are as follows: Korean patient, Seoul National University Hospital (EC); UK patient, North West-GM Central, North West Centre of REC, Manchester). Consent to publish study CT scan images is included as part of the patient's informed consent, signed by both of the patients. In the first-in-human study, a cohort size of 6 for the starting dose is standard practice, to provide sufficient safety and tolerability data about a dose level without exposing too many patients to a dose that may not be clinically beneficial. The first two patients in the starting dose cohort with an objective response were selected for inclusion in the publication. The clinical study is ongoing and further study data will be submitted for publication at a later date.

Patient Tumor Genotyping in the Trial Patient tumor tissues were analyzed for EGFR mutations using either the Qiagen EGFR RGQ PCR Kit (Cat #870111) or direct dideoxynucleotide sequencing.

Disclosure of Potential Conflicts of Interest

M.R.V. Finlay, G. Hughes, P. Ballard, T. Klinowska, S. Giorghiu, and M. Cantarini have ownership interest in AstraZeneca. D.-W. Kim is a consultant/advisory board member for Novartis and Pfizer. M.R. Ranson is a consultant/advisory board member for AstraZeneca. W. Pao reports receiving a commercial research grant from and was a consultant/advisory board member for AstraZeneca. In addition, a patent relating to EGFR^{T790M} mutation testing was licensed on behalf of W. Pao and others by Memorial Sloan Kettering Cancer Center to MolecularMD.

Authors' Contributions

Conception and design: D.A.E. Cross, S. Giorghiu, M.R.V. Finlay, R.A. Ward, P. Ballard, T. Klinowska, G.H.P. Richmond, M. Cantarini, W. Pao
Development of methodology: S. Giorghiu, C. Eberlein, J.P. Orme, V.N. Jacobs, K. Al-Kadhimi, W. Pao

Acquisition of data (provided animals, acquired and managed patients, provided facilities, etc.): S.E. Ashton, S. Giorghiu, C.A. Nebhan, P.J. Spitzler, J.P. Orme, M.J. Mellor, G. Hughes, A. Rahi, M.R. Brewer, J. Sun, H. Jin, R. Rowlinson, M. Cantarini, D.-W. Kim, W. Pao

Analysis and interpretation of data (e.g., statistical analysis, biostatistics, computational analysis): D.A.E. Cross, S.E. Ashton, S. Giorghiu, C. Eberlein, C.A. Nebhan, J.P. Orme, M.R.V. Finlay, R.A. Ward, M.J. Mellor, G. Hughes, V.N. Jacobs, M.R. Brewer, P. Ballard, K. Al-Kadhimi, R. Rowlinson, G.H.P. Richmond, M. Cantarini, W. Pao

Writing, review, and/or revision of the manuscript: D.A.E. Cross, S.E. Ashton, S. Giorghiu, C. Eberlein, C.A. Nebhan, J.P. Orme, M.R.V. Finlay, R.A. Ward, M.J. Mellor, G. Hughes, V.N. Jacobs, M.R. Brewer, P. Ballard, K. Al-Kadhimi, T. Klinowska, M. Cantarini, D.-W. Kim, M.R. Ranson, W. Pao

Administrative, technical, or material support (i.e., reporting or organizing data, constructing databases): P.J. Spitzler, J.P. Orme, A. Rahi, E. Ichihara, M.R. Ranson, W. Pao

Study supervision: S.E. Ashton, S. Giorghiu, M.J. Mellor, G. Hughes, A. Rahi, T. Klinowska, M. Cantarini, W. Pao

Acknowledgments

The authors thank the wider AstraZeneca AZD9291 project team for supporting the preclinical identification and development of AZD9291. Specifically, the authors thank Anne Galer and Paula Daunt for preclinical and clinical project team leadership; Kathryn Brown, Rik Dattani, and Joanne Wilson for assistance with drug metabolism and pharmacokinetic (DMPK) studies; Scott Martin for contribution to identification of the metabolites; Mark Anderton for leading preclinical toxicology studies; David Smith, Keith Welsh, Helen Musgrove, Vicky Sheridan, Emily Lawrie, and Paula Taylor for expert technical support; and Peter Hall for pathology input. The authors also thank Gayle Marshall, Claire Barnes, Lucy O'Brien, and Laura Ratcliffe for assistance in generating some of the resistance models and Malcom Anderson for studying AZD9291 binding to recombinant protein. At Vanderbilt, the authors thank Helen Pan for assistance with molecular genotyping assays and Daniel Colvin and Fuxue Xin for MRI assistance.

Grant Support

This work was supported by AstraZeneca. Some of this work was supported, in part, by grants from the V Foundation (to W. Pao) and the NCI (R01-CA121210, P01-CA129243, and U54-CA143798 to W. Pao). W. Pao received additional support from Vanderbilt's Specialized Program of Research Excellence in Lung Cancer grant (CA90949) and the Vanderbilt-Ingram Cancer Center Core grant (P30-CA68485). Imaging support to W. Pao was provided by NCI P30 CA68485.

The costs of publication of this article were defrayed in part by the payment of page charges. This article must therefore be hereby marked *advertisement* in accordance with 18 U.S.C. Section 1734 solely to indicate this fact.

Received March 31, 2014; revised June 1, 2014; accepted June 2, 2014; published OnlineFirst June 3, 2014.

REFERENCES

- Barker AJ, Gibson KH, Grundy W, Godfrey AA, Barlow JJ, Healy MP, et al. Studies leading to the identification of ZD1839 (IRESSA): an orally active, selective epidermal growth factor receptor tyrosine kinase inhibitor targeted to the treatment of cancer. *Bioorg Med Chem Lett* 2001;11:1911-4.
- Moyer JD, Barbacci EG, Iwata KK, Arnold L, Boman B, Cunningham A, et al. Induction of apoptosis and cell cycle arrest by CP-358,774, an inhibitor of epidermal growth factor receptor tyrosine kinase. *Cancer Res* 1997;57:4838-48.
- Lynch TJ, Bell DW, Sordella R, Gurubhagavatula S, Okimoto RA, Brannigan BW, et al. Activating mutations in the epidermal growth factor receptor underlying responsiveness of non-small-cell lung cancer to gefitinib. *N Engl J Med* 2004;350:2129-39.
- Paez JG, Janne PA, Lee JC, Tracy S, Greulich H, Gabriel S, et al. *EGFR* mutations in lung cancer: correlation with clinical response to gefitinib therapy. *Science* 2004;304:1497-500.
- Pao W, Miller V, Zakowski M, Doherty J, Politi K, Sarkaria I, et al. *EGF* receptor gene mutations are common in lung cancers from "never smokers" and are associated with sensitivity of tumors to gefitinib and erlotinib. *Proc Natl Acad Sci U S A* 2004;101:13306-11.
- Pao W, Chmielecki J. Rational, biologically based treatment of *EGFR*-mutant non-small-cell lung cancer. *Nat Rev Cancer* 2010;10:760-74.
- Maemondo M, Inoue A, Kobayashi K, Sugawara S, Oizumi S, Isobe H, et al. Gefitinib or chemotherapy for non-small-cell lung cancer with mutated *EGFR*. *N Engl J Med* 2010;362:2380-8.
- Mitsudomi T, Morita S, Yatabe Y, Negoro S, Okamoto I, Tsurutani J, et al. Gefitinib versus cisplatin plus docetaxel in patients with non-small-cell lung cancer harbouring mutations of the epidermal growth factor receptor (WJTOG3405): an open label, randomised phase 3 trial. *Lancet Oncol* 2009;11:121-8.
- Mok TS, Wu YL, Thongprasert S, Yang CH, Chu DT, Saijo N, et al. Gefitinib or carboplatin-paclitaxel in pulmonary adenocarcinoma. *N Engl J Med* 2009;361:947-57.
- Rosell R, Carcereny E, Gervais R, Vergnenegre A, Massuti B, Felip E, et al. Erlotinib versus standard chemotherapy as first-line treatment for European patients with advanced *EGFR* mutation-positive non-small-cell lung cancer (EORTC): a multicentre, open-label, randomised phase 3 trial. *Lancet Oncol* 2012;13:239-46.
- Zhou C, Wu YL, Chen G, Feng J, Liu XQ, Wang C, et al. Erlotinib versus chemotherapy as first-line treatment for patients with advanced *EGFR* mutation-positive non-small-cell lung cancer (OPTIMAL, CTONG-0802): a multicentre, open-label, randomised, phase 3 study. *Lancet Oncol* 2011;12:735-42.
- Burtress B, Anadkat M, Basti S, Hughes M, Lacouture ME, McClure JS, et al. NCCN Task Force Report: Management of dermatologic and other toxicities associated with *EGFR* inhibition in patients with cancer. *J Natl Compr Cancer Netw* 2009;7Suppl 1:S5-21.
- Takezawa K, Pirazzoli V, Arcila ME, Nebhan CA, Song X, de Stanchina E, et al. *HER2* amplification: a potential mechanism of acquired resistance to *EGFR* inhibition in *EGFR*-mutant lung cancers that lack the second-site *EGFR*T790M mutation. *Cancer Discov* 2012;2:922-33.
- Bean J, Brennan C, Shih JY, Riely G, Viale A, Wang L, et al. *MET* amplification occurs with or without T790M mutations in *EGFR* mutant lung tumors with acquired resistance to gefitinib or erlotinib. *Proc Natl Acad Sci U S A* 2007;104:20932-7.
- Engelman JA, Zejnullahu K, Mitsudomi T, Song Y, Hyland C, Park JO, et al. *MET* amplification leads to gefitinib resistance in lung cancer by activating *ERBB3* signaling. *Science* 2007;316:1039-43.
- Sequist LV, Waltman BA, Dias-Santagata D, Digumarthy S, Turke AB, Fidias P, et al. Genotypic and histological evolution of lung cancers acquiring resistance to *EGFR* inhibitors. *Sci Transl Med* 2011;3:75ra26.
- Ohashi K, Sequist LV, Arcila ME, Moran T, Chmielecki J, Lin YL, et al. Lung cancers with acquired resistance to *EGFR* inhibitors occasionally harbor *BRAF* gene mutations but lack mutations in *KRAS*, *NRAS*, or *MEK1*. *Proc Natl Acad Sci U S A* 2012;109:E2127-33.
- de Bruin EC, Cowell CF, Warne PH, Jiang M, Saunders RE, Melnick MA, et al. Reduced *NF1* expression confers resistance to *EGFR* inhibition in lung cancer. *Cancer Discov* 2014;4:606-19.
- Ware KE, Marshall ME, Heasley LR, Marek L, Hinz TK, Hercule P, et al. Rapidly acquired resistance to *EGFR* tyrosine kinase inhibitors in NSCLC cell lines through de-repression of *FGFR2* and *FGFR3* expression. *PLoS ONE* 2010;5:e14117.
- Kobayashi S, Boggon TJ, Dayaram T, Janne PA, Kocher O, Meyerson M, et al. *EGFR* mutation and resistance of non-small-cell lung cancer to gefitinib. *N Engl J Med* 2005;352:786-92.
- Pao W, Miller VA, Politi KA, Riely GJ, Somwar R, Zakowski MF, et al. Acquired resistance of lung adenocarcinomas to gefitinib or erlotinib is associated with a second mutation in the *EGFR* kinase domain. *PLoS Med* 2005;2:e73.
- Sos ML, Rode HB, Heynck S, Peifer M, Fischer F, Kluter S, et al. Chemogenomic profiling provides insights into the limited activity of irreversible *EGFR* inhibitors in tumor cells expressing the T790M *EGFR* resistance mutation. *Cancer Res* 2010;70:868-74.
- Yun CH, Mengwasser KE, Toms AV, Woo MS, Greulich H, Wong KK, et al. The T790M mutation in *EGFR* kinase causes drug resistance by increasing the affinity for ATP. *Proc Natl Acad Sci U S A* 2008;105:2070-5.
- Li D, Ambrogio L, Shimamura T, Kubo S, Takahashi M, Chirieac LR, et al. BIBW2992, an irreversible *EGFR*/*HER2* inhibitor highly effective in preclinical lung cancer models. *Oncogene* 2008;27:4702-11.
- Engelman JA, Zejnullahu K, Gale CM, Lifshits E, Gonzales AJ, Shimamura T, et al. PF00299804, an irreversible pan-*ERBB* inhibitor, is effective in lung cancer models with *EGFR* and *ERBB2* mutations that are resistant to gefitinib. *Cancer Res* 2007;67:11924-32.
- Ramalingam SS, Blackhall F, Krzakowski M, Barrios CH, Park K, Bover I, et al. Randomized phase II study of dacomitinib (PF-00299804), an irreversible pan-human epidermal growth factor receptor inhibitor, versus erlotinib in patients with advanced non-small-cell lung cancer. *J Clin Oncol* 2012;30:3337-44.

27. Sequist LV, Yang JC, Yamamoto N, O'Byrne K, Hirsh V, Mok T, et al. Phase III study of afatinib or cisplatin plus pemetrexed in patients with metastatic lung adenocarcinoma with EGFR mutations. *J Clin Oncol* 2013;31:3327–34.
28. Miller VA, Hirsh V, Cadranel J, Chen YM, Park K, Kim SW, et al. Afatinib versus placebo for patients with advanced, metastatic non-small-cell lung cancer after failure of erlotinib, gefitinib, or both, and one or two lines of chemotherapy (LUX-Lung 1): a phase 2b/3 randomised trial. *Lancet Oncol* 2012;13:528–38.
29. Katakami N, Atagi S, Goto K, Hida T, Horai T, Inoue A, et al. LUX-lung 4: a phase II trial of afatinib in patients with advanced non-small-cell lung cancer who progressed during prior treatment with erlotinib, gefitinib, or both. *J Clin Oncol* 2013;31:3335–41.
30. Eskens FA, Mom CH, Planting AS, Gietema JA, Amelsberg A, Huisman H, et al. A phase I dose escalation study of BIBW 2992, an irreversible dual inhibitor of epidermal growth factor receptor 1 (EGFR) and 2 (HER2) tyrosine kinase in a 2-week on, 2-week off schedule in patients with advanced solid tumours. *Br J Cancer* 2008;98:80–5.
31. Chmielecki J, Foo J, Oxnard GR, Hutchinson K, Ohashi K, Somwar R, et al. Optimization of dosing for EGFR-mutant non-small cell lung cancer with evolutionary cancer modeling. *Sci Transl Med* 2011;3:90ra59.
32. Kim Y, Ko J, Cui Z, Abolhoda A, Ahn JS, Ou SH, et al. The EGFR T790M mutation in acquired resistance to an irreversible second-generation EGFR inhibitor. *Mol Cancer Ther* 2012;11:784–91.
33. Janjigian YY, Smit EF, Groen HJM, Horn L, Gettinger S, Camidge DR, et al. Dual inhibition of EGFR with afatinib and cetuximab in kinase inhibitor-resistant EGFR-mutant lung cancer with and without T790M Mutations. *Cancer Discov* 2014;4:1036–45.
34. Zhou W, Ercan D, Chen L, Yun CH, Li D, Capelletti M, et al. Novel mutant-selective EGFR kinase inhibitors against EGFR T790M. *Nature* 2009;462:1070–4.
35. Walter AO, Sjin RT, Haringsma HJ, Ohashi K, Sun J, Lee K, et al. Discovery of a mutant-selective covalent inhibitor of EGFR that overcomes T790M-mediated resistance in NSCLC. *Cancer Discov* 2013;3:1404–15.
36. Ward RA, Anderton MJ, Ashton S, Bethel PA, Box M, Butterworth S, et al. Structure- and reactivity-based development of covalent inhibitors of the activating and gatekeeper mutant forms of the epidermal growth factor receptor (EGFR). *J Med Chem* 2013;56:7025–48.
37. Red Brewer M, Yun C-H, Lai D, Lemmon MA, Eck MJ, Pao W. Mechanism for activation of mutated epidermal growth factor receptors in lung cancer. *Proc Natl Acad Sci U S A* 2013;110:E3595–604.
38. Sos ML, Koker M, Weir BA, Heynck S, Rabinovsky R, Zander T, et al. PTEN loss contributes to erlotinib resistance in EGFR-mutant lung cancer by activation of Akt and EGFR. *Cancer Res* 2009;69:3256–61.
39. Chmielecki J, Pietanza MC, Aftab D, Shen R, Zhao Z, Chen X, et al. EGFR-mutant lung adenocarcinomas treated first-line with the novel EGFR inhibitor, XL647, can subsequently retain moderate sensitivity to erlotinib. *J Thoracic Oncol* 2012;7:434–42.
40. Hickinson DM, Klinowska T, Speake G, Vincent J, Trigwell C, Anderton J, et al. AZD8931, an equipotent, reversible inhibitor of signaling by epidermal growth factor receptor, ERBB2 (HER2), and ERBB3: a unique agent for simultaneous ERBB receptor blockade in cancer. *Clin Cancer Res* 2010;16:1159–69.
41. Wong AJ, Ruppert JM, Bigner SH, Grzeschik CH, Humphrey PA, Bigner DS, et al. Structural alterations of the epidermal growth factor receptor gene in human gliomas. *Proc Natl Acad Sci U S A* 1992;89:2965–9.
42. Shigematsu H, Takahashi T, Nomura M, Majumdar K, Suzuki M, Lee H, et al. Somatic mutations of the HER2 kinase domain in lung adenocarcinomas. *Cancer Res* 2005;65:1642–6.
43. Wang SE, Narasanna A, Perez-Torres M, Xiang B, Wu FY, Yang S, et al. HER2 kinase domain mutation results in constitutive phosphorylation and activation of HER2 and EGFR and resistance to EGFR tyrosine kinase inhibitors. *Cancer Cell* 2006;10:25–38.
44. Merlino GT, Xu YH, Ishii S, Clark AJ, Semba K, Toyoshima K, et al. Amplification and enhanced expression of the epidermal growth factor receptor gene in A431 human carcinoma cells. *Science* 1984;224:417–9.
45. Politi K, Zakowski MF, Fan PD, Schonfeld EA, Pao W, Varmus HE. Lung adenocarcinomas induced in mice by mutant EGF receptors found in human lung cancers respond to a tyrosine kinase inhibitor or to down-regulation of the receptors. *Genes Dev* 2006;20:1496–510.
46. Regales L, Balak MN, Gong Y, Politi K, Sawai A, Le C, et al. Development of new mouse lung tumor models expressing EGFR T790M mutants associated with clinical resistance to kinase inhibitors. *PLoS ONE* 2007;2:e810.
47. Regales L, Gong Y, Shen R, de Stanchina E, Vivanco I, Goel A, et al. Dual targeting of EGFR can overcome a major drug resistance mutation in mouse models of EGFR mutant lung cancer. *J Clin Invest* 2009;119:3000–10.
48. Eisenhauer EA, Therasse P, Bogaerts J, Schwartz LH, Sargent D, Ford R, et al. New response evaluation criteria in solid tumours: revised RECIST guideline (version 1.1). *Eur J Cancer* 2009;45:228–47.
49. Ranson M, Pao W, Kim D-W, Kim S-W, Ohe Y, Felip E, et al. Preliminary results from a Phase I study with AZD9291: an irreversible inhibitor of epidermal growth factor receptor (EGFR) activating and resistance mutations in non-small cell lung cancer (NSCLC). *Eur J Cancer* 2013;49(suppl 3; abstr LBA33):S15.
50. Jackman D, Pao W, Riely GJ, Engelman JA, Kris MG, Janne PA, et al. Clinical definition of acquired resistance to epidermal growth factor receptor tyrosine kinase inhibitors in non-small-cell lung cancer. *J Clin Oncol* 2010;28:357–60.
51. Ranson M, Pao W, Kim D-W, Kim S-W, Ohe Y, Felip E, et al. AZD9291: an irreversible, potent and selective tyrosine kinase inhibitor (TKI) of activating (EGFRm+) and resistance (T790M) mutations in advanced NSCLC. *J Thorac Oncol* 2013;8(Suppl 2; abstract MO21.12):S389.
52. Sequist LV, Soria JC, Gadgeel SM, Wakelee HA, Camidge DR, Varga A, et al. First-in-human evaluation of CO-1686, an irreversible, selective, and potent tyrosine kinase inhibitor of EGFR T790M. *J Clin Oncol* 2013;31(suppl; abstr 2524).
53. Soria JC, Sequist LV, Gadgeel S, Goldman J, Wakelee H, Varga A, et al. First-in-human evaluation of CO-1686, an irreversible, highly selective tyrosine kinase inhibitor of mutations of EGFR (activating and T790M). *J Thoracic Oncol* 2013;8(Suppl 2; abstr O03.06):S141.
54. Sequist LV, Martins RG, Spigel D, Grunberg SM, Spira A, Janne PA, et al. First-line gefitinib in patients with advanced non-small-cell lung cancer harboring somatic EGFR mutations. *J Clin Oncol* 2008;26:2442–9.
55. Costa C, Molina-Vila MA, Drozdowskyj A, Gimenez-Capitan A, Bertran-Alamillo J, Karachaliou N, et al. The impact of EGFR T790M mutations and BIM mRNA expression on outcome in patients with EGFR-mutant NSCLC treated with erlotinib or chemotherapy in the randomized phase III EORTC trial. *Clin Cancer Res* 2014;20:2001–10.
56. Ye X, Zhu ZZ, Zhong L, Lu Y, Sun Y, Yin X, et al. High T790M detection rate in TKI-naïve NSCLC with EGFR sensitive mutation: truth or artifact? *J Thorac Oncol* 2013;8:1118–20.
57. Porta R, Sanchez-Torres JM, Paz-Ares L, Massuti B, Reguart N, Mayo C, et al. Brain metastases from lung cancer responding to erlotinib: the importance of EGFR mutation. *Eur Respir J* 2011;37:624–31.
58. McKillop D, Hutchison M, Partridge EA, Bushby N, Cooper CMF, Clarkson-Jones JA, et al. Metabolic disposition of gefitinib, an epidermal growth factor receptor tyrosine kinase inhibitor, in rat, dog and man. *Xenobiotica* 2004;34:917–34.
59. Cortot AB, Repellin CE, Shimamura T, Capelletti M, Zejnullahu K, Ercan D, et al. Resistance to irreversible EGF receptor tyrosine kinase inhibitors through a multistep mechanism involving the IGF1R pathway. *Cancer Res* 2013;73:834–43.
60. Ercan D, Xu C, Yanagita M, Monast CS, Pratilas CA, Montero J, et al. Reactivation of ERK signaling causes resistance to EGFR kinase inhibitors. *Cancer Discov* 2012;2:934–47.
61. Su Z, Dias-Santagata D, Duke M, Hutchinson K, Lin YL, Borger DR, et al. A platform for rapid detection of multiple oncogenic mutations with relevance to targeted therapy in non-small-cell lung cancer. *J Mol Diagn* 2011;13:74–84.